

# An improved return-mapping scheme for nonsmooth yield surfaces: PART I - the Haigh-Westergaard coordinates

S. Sysala<sup>1</sup>, M. Cermak<sup>1,2</sup>, T. Koudelka<sup>3</sup>, J. Kruis<sup>3</sup>, J. Zeman<sup>2,3</sup>, R. Blaheta<sup>1</sup>

<sup>1</sup>Institute of Geonics CAS, Ostrava, Czech Republic

<sup>2</sup>VŠB–Technical University of Ostrava, Ostrava, Czech Republic

<sup>3</sup>Czech Technical University in Prague, Prague, Czech Republic

August 24, 2021

## Abstract

The paper is devoted to the numerical solution of elastoplastic constitutive initial value problems. An improved form of the implicit return-mapping scheme for nonsmooth yield surfaces is proposed that systematically builds on a subdifferential formulation of the flow rule. The main advantage of this approach is that the treatment of singular points, such as apices or edges at which the flow direction is multivalued involves only a uniquely defined set of non-linear equations, similarly to smooth yield surfaces. This paper (PART I) is focused on isotropic models containing: *a*) yield surfaces with one or two apices (singular points) laying on the hydrostatic axis; *b*) plastic pseudo-potentials that are independent of the Lode angle; *c*) nonlinear isotropic hardening (optionally). It is shown that for some models the improved integration scheme also enables to a priori decide about a type of the return and investigate existence, uniqueness and semismoothness of discretized constitutive operators in implicit form. Further, the semismooth Newton method is introduced to solve incremental boundary-value problems. The paper also contains numerical examples related to slope stability with available Matlab implementation.

Keywords: elastoplasticity, nonsmooth yield surface, multivalued flow direction, implicit return-mapping scheme, semismooth Newton method, limit analysis

## 1 Introduction

The paper is devoted to the numerical solution of small-strain quasi-static elastoplastic problems. Such a problem consists of the constitutive initial value problem (CIVP) and the balance equation representing the principle of virtual work. A broadly exploited and universal numerical/computational concept includes the following steps:

- (a) time-discretization of CIVP leading to an incremental constitutive problem;
- (b) derivation of the constitutive and consistent tangent operators;
- (c) substitution of the constitutive (stress-strain) operator into the balance equation leading to the incremental boundary value problem in terms of displacements;
- (d) finite element discretization and derivation of a system of nonlinear equations;
- (e) solving the system using a nonsmooth variant of the Newton method.

CIVP satisfies thermodynamical laws and usually involves internal variables such as plastic strains or hardening parameters. Several integration schemes for numerical solution of CIVP were suggested. For their overview, we refer, e.g., [9, 11, 32, 33] and references introduced therein. If the implicit or trapezoidal Euler method is used then the incremental constitutive problem is solved by the elastic predictor/plastic corrector method. The plastic correction leads to the return-mapping scheme. We distinguish, e.g., implicit, trapezoidal or midpoint return-mappings depending on a chosen time-discretization [11, Chapter 7].

In this paper, we assume that the plastic flow direction is generated by the plastic potential,  $g$ . If  $g$  is smooth then the corresponding plastic flow direction is uniquely determined by the derivative of  $g$  and consequently, the plastic flow rule reads as follows, e.g. [11, Chapter 8]:

$$\dot{\boldsymbol{\epsilon}}^p = \dot{\lambda} \frac{\partial g(\boldsymbol{\sigma}, A)}{\partial \boldsymbol{\sigma}}, \quad g = g(\boldsymbol{\sigma}, A). \quad (1.1)$$

Here,  $\dot{\boldsymbol{\epsilon}}^p$ ,  $\dot{\lambda}$ ,  $\boldsymbol{\sigma}$ , and  $A$  denotes the plastic strain rate, the plastic multiplier rate, the stress tensor and the hardening thermodynamical forces, respectively. The corresponding return-mapping scheme is relatively straightforward and leads to solving a system of nonlinear equations. A difficulty arises when  $g$  is *nonsmooth*. Mostly, it happens if the yield surface contains singular points, such as apices or edges. Then the function  $g$  is rather pseudo-potential than potential and its derivative need not exist everywhere. In such a case, the rule (1.1) is usually completed by some additive formulas depending on particular cases of  $g$  and  $\boldsymbol{\sigma}$  in an ad-hoc manner. For example, the implementation of the Mohr-Coulomb model reported in [11, Chapter 6, 8] employs one, two, or six plastic multipliers  $\lambda$ , depending on the location of  $\boldsymbol{\sigma}$  on the yield surface. Since the stress tensor  $\boldsymbol{\sigma}$  is unknown in CIVP one must blindly guess its right location. Moreover, for each tested location, one must usually solve an auxiliary system of nonlinear equations whose solvability is not guaranteed in general. *These facts are evident drawbacks of the current return-mapping schemes.*

In associative plasticity, it is well-known that the plastic flow rule (1.1) together with a hardening law and loading/unloading conditions can be equivalently replaced by the principle of maximum plastic dissipation within the constitutive model. This alternative formulation of CIVP does not require special treatment for nonsmooth  $g$  and enables to solve CIVP by techniques based on mathematical programming [5, 13, 29]. In particular, if the implicit or trapezoidal Euler method is used then the incremental constitutive problem can be interpreted by a certain kind of the closest-point projection [3, 27, 36]. For some nonassociative models, CIVP can be re-formulated using a theory of bipotentials that leads to new numerical schemes [10, 20, 40]. These alternative definitions of the flow rule enable a variational re-formulation of the initial boundary value elastoplastic problem. Consequently, solvability of this problem can be investigated (see, e.g., [18, 24]). Therefore, the corresponding numerical techniques are usually also correct from the mathematical point of view. On the other hand, such a numerical treatment is not so universal and its implementation is more involved/too complex in comparison with standard procedures of computational inelasticity.

The approach pursued in this paper builds on the subdifferential formulation of the plastic flow rule, e.g. [11, Section 6.3.9],

$$\dot{\boldsymbol{\epsilon}}^p \in \dot{\lambda} \partial_{\boldsymbol{\sigma}} g(\boldsymbol{\sigma}, A) \quad (1.2)$$

for nonsmooth  $g$ . Here,  $\partial_{\boldsymbol{\sigma}} g(\boldsymbol{\sigma}, A)$  denotes the subdifferential of  $g$  at  $(\boldsymbol{\sigma}, A)$  with respect to the stress variable. If  $g$  is convex at least in vicinity of the yield surface then this definition is justified, e.g., by [30, Corollary 23.7.1] and is valid even when  $g$  is not smooth at  $\boldsymbol{\sigma}$ . On the first sight, it seems that (1.2) is not convenient for numerical treatment due to the presence of the multivalued flow direction. The main goal of this paper is to show that the *opposite is true*, by demonstrating that the implicit return-mapping scheme based on (1.2) leads to solving a just one system of nonlinear equations regardless whether the unknown stress tensor lies on the smooth portion of the yield surface or not at least for a wide class of models with nonsmooth plastic pseudo-potentials. Using this technique, we eliminate the blind guessing and thus considerably simplify the solution scheme. Moreover, the new

technique enables to investigate some useful properties of the constitutive operator, like uniqueness or semismoothness, that are not obvious for the current technique.

## 1.1 Basic idea

First of all, we illustrate the new technique on a simple 2D projective problem that mimics the structure of an incremental elastoplastic constitutive problem. Consider the convex set

$$B := \{\mathbf{w} = (w_1, w_2) \in \mathbb{R}^2 \mid f(\mathbf{w}) \leq 0\}, \quad f(\mathbf{w}) := w_1 + |w_2| - 1,$$

and define the projection  $\mathbf{w}^* \in B$  of a point  $\mathbf{z} = (z_1, z_2) \in \mathbb{R}^2$  as follows:

$$\|\mathbf{z} - \mathbf{w}^*\|^2 = \min_{\mathbf{w} \in B} \|\mathbf{z} - \mathbf{w}\|^2, \quad \|\mathbf{z}\|^2 := z_1^2 + z_2^2.$$

The scheme of the projection is depicted in Figure 1.

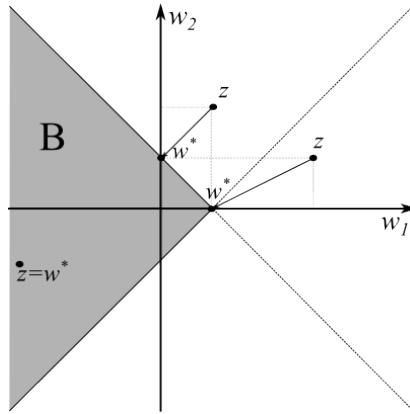


Figure 1: Scheme of the projection.

Clearly, the function  $f$  is convex in  $\mathbb{R}^2$ , nondifferentiable at  $\mathbf{w} = (w_1, 0)$  and

$$\nabla f(\mathbf{w}) = \left(1, \frac{w_2}{|w_2|}\right)^T \in \mathbb{R}^2 \quad \forall \mathbf{w} = (w_1, w_2), \quad w_2 \neq 0. \quad (1.3)$$

If  $\mathbf{z} \in B$  then  $\mathbf{w}^* = \Pi_B(\mathbf{z}) = \mathbf{z}$ . Conversely, if  $\mathbf{z} \notin B$  it follows from the Karush-Kuhn-Tucker conditions and (1.3) that the projective problem can be written as follows: *find*  $\mathbf{w}^* = (w_1^*, w_2^*)^T \in \mathbb{R}^2$  *and the Lagrange multiplier*  $\lambda > 0$ :

$$z_1 - w_1^* = \lambda, \quad z_2 - w_2^* \in \lambda \partial |w_2^*|, \quad w_1^* + |w_2^*| - 1 = 0, \quad (1.4)$$

where

$$\partial |w_2^*| = \begin{cases} \{w_2^*/|w_2^*|\}, & w_2^* \neq 0, \\ [-1, 1], & w_2^* = 0, \end{cases}$$

To find a solution to (1.4), it is crucial to rewrite the inclusion (1.4)<sub>2</sub> as an equation. Observe that

$$z_2 - w_2^* \in \lambda \partial |w_2^*| \quad \text{if and only if} \quad w_2^* = (|z_2| - \lambda)^+ \frac{z_2}{|z_2|},$$

where  $(\cdot)^+$  denotes a positive part of a function. This crucial transformation will be derived in detail in Section 3 on an analogous elastoplastic example. Thus (1.4) leads to the following system of equations:

$$w_1^* = z_1 - \lambda, \quad w_2^* = (|z_2| - \lambda)^+ \frac{z_2}{|z_2|}, \quad w_1^* + |w_2^*| - 1 = 0, \quad (1.5)$$

Since (1.5)<sub>2</sub> implies  $|w_2^*| = (|z_2| - \lambda)^+$ , the system of three nonlinear equations reduces to a single one

$$z_1 - \lambda + (|z_2| - \lambda)^+ - 1 = 0.$$

Consequently,  $\lambda$  can be found in the closed form as

$$\lambda = z_1 - 1 + \frac{1}{2}(-z_1 + |z_2| + 1)^+ = \begin{cases} \frac{1}{2}(z_1 + |z_2| - 1), & z_1 - |z_2| - 1 \leq 0, \\ z_1 - 1, & z_1 - |z_2| - 1 \geq 0 \end{cases}$$

from which one can easily compute  $\mathbf{w}^* = (w_1^*, w_2^*)^T$  by (1.5)<sub>1</sub> and (1.5)<sub>2</sub>.

## 1.2 Content of the the paper

The presented idea is systematically extended on some elastoplastic models. This paper, PART I, is focused on isotropic models containing: *a*) yield surfaces with one or two apices (singular points) laying on the hydrostatic axis; *b*) plastic pseudo-potentials that are independent of the Lode angle; *c*) nonlinear isotropic hardening (optionally). Such models are usually formulated by the Haigh-Westergaard coordinates. Further, the implicit Euler discretization of CIVP is considered and thus two types of return on the yield surface within the plastic correction are distinguished: *(i)* return to the smooth portion of the yield surface; *(ii)* return to the apex (apices).

The paper is organized as follows. Section 2 contains some preliminaries related to invariants of the stress tensor and semismooth functions. Section 3 is devoted to the Drucker-Prager model including the nonlinear isotropic hardening. Although the plastic corrector cannot be found in closed form, the new technique enables to a priori decide about the return type and prove existence, uniqueness and semismoothness of the implicit constitutive operator. The consistent tangent operator is also introduced. In Section 4, we derive similar results for the perfect plastic part of the Jirásek-Grassl model [15]. In Section 5, the new technique is extended on an abstract model written by the Haigh-Westergaard coordinates. In particular, within the plastic correction, we formulate a unique system of nonlinear equations which is common for the both type of the return. It can lead to a more correct and/or simpler solution scheme in comparison with the current technique. Section 6 is devoted to numerical realization of the incremental boundary value elastoplastic problem using the semismooth Newton method. In Section 7, illustrative numerical examples related to a slope stability benchmark are considered. Here, limit load is analyzed by an incremental method depending on a mesh type and mesh density for the Drucker-Prager and Jirásek-Grassl models.

Within this paper, second order tensors, matrices and vectors are denoted by bold letters. As usual, small letters are used for vectors and capitals for matrices (see Section 6). Further, the fourth order tensors are denoted by capital blackboard letters, e.g.,  $\mathbb{D}_e$  or  $\mathbb{I}_{dev}$ . The symbol  $\otimes$  means the tensor product [11, 17]. We also use the following notation:  $\mathbb{R}_+ := \{z \in \mathbb{R}; z \geq 0\}$  and  $\mathbb{R}_{sym}^{3 \times 3}$  for the space of symmetric, second order tensors.

## 2 Preliminaries

### 2.1 Invariants of a stress tensor and their derivatives

Consider a stress tensor  $\boldsymbol{\sigma} \in \mathbb{R}_{sym}^{3 \times 3}$  and its splitting into the volumetric and deviatoric parts:

$$\boldsymbol{\sigma} = p\mathbf{I} + \mathbf{s}, \quad p := p(\boldsymbol{\sigma}) = \frac{1}{3}\mathbf{I} : \boldsymbol{\sigma}, \quad \mathbf{s} := \mathbf{s}(\boldsymbol{\sigma}) = \mathbb{I}_{dev} : \boldsymbol{\sigma} = \boldsymbol{\sigma} - \frac{1}{3}(\mathbf{I} : \boldsymbol{\sigma})\mathbf{I}.$$

Here,  $\mathbf{I}$ ,  $\mathbb{I}_{dev}$ ,  $p$  and  $\mathbf{s}$  denote the identity second order tensor, the fourth order deviatoric projection tensor, the hydrostatic pressure, and the deviatoric stress, respectively. *The Haigh-Westergaard coordinates* are created by the invariants  $p$ ,  $\varrho$  and  $\theta$ , where

$$\varrho := \varrho(\boldsymbol{\sigma}) = \sqrt{\mathbf{s} : \mathbf{s}} = \|\mathbf{s}\|,$$

$$\theta := \theta(\boldsymbol{\sigma}) = \frac{1}{3} \arccos \left( \frac{3\sqrt{3}}{2} \frac{J_3}{J_2^{3/2}} \right), \quad J_2(\mathbf{s}) = \frac{1}{2} \mathbf{s} : \mathbf{s} = \frac{1}{2} \varrho^2, \quad J_3(\mathbf{s}) = \frac{1}{3} \mathbf{s}^3 : \mathbf{I}, \quad \mathbf{s} := \mathbf{s}(\boldsymbol{\sigma}).$$

Clearly,  $\varrho \geq 0$  and  $\theta \in [0, \pi/3]$ . Since  $\theta$  is not well-defined when  $\varrho = 0$ , the Lode angle is included in elastoplastic models indirectly. Usually, it is considered another invariant in the form

$$\tilde{\varrho} := \tilde{\varrho}(\boldsymbol{\sigma}) = \varrho \tilde{r}(\cos \theta), \quad (2.1)$$

where  $\tilde{r}(\cdot)$  is assumed to be a smooth function such that  $\tilde{\varrho}(\cdot)$  is at least continuous. However, as we will see below, it is more convenient to assume *strong semismoothness* of  $\tilde{\varrho}(\cdot)$ . As a particular case, it will be considered the invariant

$$\varrho_e := \varrho_e(\boldsymbol{\sigma}) = \varrho r_e(\cos \theta), \quad (2.2)$$

where

$$r_e(\cos \theta) = \frac{4(1 - e^2) \cos^2 \theta + (2e - 1)^2}{2(1 - e^2) \cos \theta + (2e - 1) \sqrt{4(1 - e^2) \cos^2 \theta + 5e^2 - 4e}}. \quad (2.3)$$

The function  $r_e$  was proposed in [39] and contains the excentricity parameter  $e \in [0.5, 1]$ . It holds: a)  $r_e(\cos \theta(\cdot))$  is a bounded and smooth function for any  $\boldsymbol{\sigma} \in \mathbb{R}_{sym}^{3 \times 3}$ ,  $\varrho(\boldsymbol{\sigma}) > 0$ ; b)  $\varrho_e(\boldsymbol{\sigma}) = 0$  when  $\varrho = 0$ ; c)  $\varrho_e = \varrho$ ,  $r_e(\cos \theta) = 1$  when  $e = 1$ .

We will also use the following derivatives:

$$\frac{\partial p}{\partial \boldsymbol{\sigma}} = \frac{\mathbf{I}}{3}, \quad \frac{\partial \mathbf{s}}{\partial \boldsymbol{\sigma}} = \mathbb{I}_{dev}, \quad \mathbf{n}(\boldsymbol{\sigma}) := \frac{\partial \varrho}{\partial \boldsymbol{\sigma}} = \frac{\mathbf{s}}{\varrho}, \quad \frac{\partial \mathbf{n}}{\partial \boldsymbol{\sigma}} = \frac{1}{\varrho} (\mathbb{I}_{dev} - \mathbf{n} \otimes \mathbf{n}), \quad (2.4)$$

$$\frac{\partial \theta}{\partial \boldsymbol{\sigma}} = \frac{\sqrt{6}}{\varrho \sin(3\theta)} [(\mathbf{n} \otimes \mathbf{n}^3) \mathbf{I} - \mathbb{I}_{dev}(\mathbf{n}^2)], \quad \frac{\partial r_e}{\partial \boldsymbol{\sigma}} = -r'_e(\cos \theta) \sin \theta \frac{\partial \theta}{\partial \boldsymbol{\sigma}}. \quad (2.5)$$

Notice that the derivatives of  $\varrho$ ,  $\mathbf{n}$ ,  $\theta$  and  $r_e$  do not exist when  $\varrho = 0$ . Further,  $\theta$  is not differentiable when  $\boldsymbol{\sigma}$  satisfies either  $\theta = 0$  or  $\theta = \pi/3$ . On the other hand,  $r_e$  has derivatives for such stresses [39].

For purposes of this paper, it is crucial to derive the subdifferential of  $\varrho$  at  $\boldsymbol{\sigma}$  when  $\varrho(\boldsymbol{\sigma}) = 0$ :

$$\begin{aligned} \partial \varrho(\boldsymbol{\sigma}) &= \{ \hat{\mathbf{n}} \in \mathbb{R}_{sym}^{3 \times 3} \mid \varrho(\boldsymbol{\tau}) \geq \varrho(\boldsymbol{\sigma}) + \hat{\mathbf{n}} : (\boldsymbol{\tau} - \boldsymbol{\sigma}) \quad \forall \boldsymbol{\tau} \in \mathbb{R}_{sym}^{3 \times 3} \} \\ &= \{ \hat{\mathbf{n}} \in \mathbb{R}_{sym}^{3 \times 3} \mid \|\mathbf{s}(\boldsymbol{\tau})\| \geq (\hat{\mathbf{n}} : \mathbf{I})(p(\boldsymbol{\tau}) - p(\boldsymbol{\sigma})) + \hat{\mathbf{n}} : \mathbf{s}(\boldsymbol{\tau}) \quad \forall \boldsymbol{\tau} \in \mathbb{R}_{sym}^{3 \times 3} \} \\ &= \{ \hat{\mathbf{n}} \in \mathbb{R}_{sym}^{3 \times 3} \mid \mathbf{I} : \hat{\mathbf{n}} = 0, \quad \|\mathbf{s}(\boldsymbol{\tau})\| \geq \hat{\mathbf{n}} : \mathbf{s}(\boldsymbol{\tau}) \quad \forall \boldsymbol{\tau} \in \mathbb{R}_{sym}^{3 \times 3} \} \\ &= \{ \hat{\mathbf{n}} \in \mathbb{R}_{sym}^{3 \times 3} \mid \mathbf{I} : \hat{\mathbf{n}} = 0, \quad \|\hat{\mathbf{n}}\| \leq 1 \} \quad \text{if } \varrho(\boldsymbol{\sigma}) = 0. \end{aligned} \quad (2.6)$$

If  $\varrho(\boldsymbol{\sigma}) > 0$  then  $\partial \varrho(\boldsymbol{\sigma}) = \{ \mathbf{n}(\boldsymbol{\sigma}) \}$  by (2.4)<sub>3</sub>. It is readily seen that

$$\mathbf{I} : \hat{\mathbf{n}} = 0 \quad \forall \hat{\mathbf{n}} \in \partial \varrho(\boldsymbol{\sigma}), \quad (2.7)$$

regardless  $\varrho(\boldsymbol{\sigma}) = 0$  or not.

## 2.2 Semismooth functions

Semismoothness was originally introduced by Mifflin [25] for functionals. Qi and J. Sun [28] extended the definition of semismoothness to vector-valued functions to investigate the superlinear convergence of the Newton method. We introduce a definition of *strongly semismooth* functions [34, 14, 26]. To this end, consider finite dimensional spaces  $X$  and  $Y$  with the norms  $\|\cdot\|_X$  and  $\|\cdot\|_Y$ , respectively. In the context of this paper, the abstract spaces  $X, Y$  represent either subspaces of  $\mathbb{R}^n$  or the space  $\mathbb{R}_{sym}^{3 \times 3}$ .

**Definition 2.1.** Let  $F : X \rightarrow Y$  be locally Lipschitz function in a neighborhood of some  $x \in X$  and  $\partial F(x)$  denote the generalized Jacobian in the Clarke sense [8]. We say that  $F$  is strongly semismooth at  $x$  if

- (i)  $F$  is directionally differentiable at  $x$ ,
- (ii) for any  $h \in X$ ,  $h \rightarrow 0$ , and any  $V \in \partial F(x+h)$ ,

$$F(x+h) - F(x) - Vh = O(\|h\|_X^2). \quad (2.8)$$

Notice that the estimate (2.8) is called the quadratic approximate property in [34] or the strong  $G$ -semismoothness in [14, 26]. In literature, there exists several equivalent definitions of strongly semismooth functions, see [28, 34]. For example the condition (2.8) can be replaced with

$$F'(x+h;h) - F'(x;h) = O(\|h\|_X^2) \quad \forall h \in X, h \rightarrow 0, x+h \in \mathcal{D}_F, \quad (2.9)$$

where  $\mathcal{D}_F$  is the subset of  $X$ ,  $F$  is Fréchet differentiable and  $F'(x;h)$  denotes the directional derivative of  $F$  at a point  $x$  and a direction  $h$ . We say that  $F : X \rightarrow Y$  is strongly semismooth on an open set  $\mathcal{O} \subset X$  if  $F$  is strongly semismooth at every point of  $\mathcal{O}$ .

Since it is difficult to straightforwardly prove (2.8) or (2.9), we summarize several auxilliary results. Firstly, piecewise smooth ( $PC^1$ ) functions with Lipschitz continuous derivatives of selected functions belong among strongly semismooth functions [12]. Especially, we mention the max-function,  $\xi : \mathbb{R} \rightarrow \mathbb{R}$ ,  $\xi(s) = \max\{0, s\} = s^+$ . Further, scalar product, sum, compositions of strongly semismooth functions are strongly semismooth. Finally, we will use the following version of the implicit function theorem [8, 34, 23].

**Theorem 2.1.** Let  $\mathcal{I} : Y \times X \rightarrow X$  be a locally Lipschitz function in a neighborhood of  $(\bar{y}, \bar{x})$ , which solve  $\mathcal{I}(\bar{y}, \bar{x}) = 0$ . Let  $\partial_x \mathcal{I}(y, x)$  denote the generalized derivatives of  $\mathcal{I}$  at  $(y, x)$  with respect to the variables  $x$ . If  $\partial_x \mathcal{I}(\bar{y}, \bar{x})$  is of maximal rank, i.e. the following implication holds,

$$\mathcal{I}_x^o \Delta x = 0, \mathcal{I}_x^o \in \partial_x \mathcal{I}(\bar{y}, \bar{x}) \implies \Delta x = 0, \quad (2.10)$$

then there exists an open neighborhood  $\mathcal{O}_{\bar{y}}$  of  $\bar{y}$  and a function  $F : \mathcal{O}_{\bar{y}} \rightarrow X$  such that  $F$  is locally Lipschitz continuous in  $\mathcal{O}_{\bar{y}}$ ,  $F(\bar{y}) = \bar{x}$  and for every  $y$  in  $\mathcal{O}_{\bar{y}}$ ,  $\mathcal{I}(y, F(y)) = 0$ .

Moreover, if  $\mathcal{I}$  is strongly semismooth at  $(\bar{y}, \bar{x})$ , then  $F$  strongly semismooth at  $\bar{y}$ .

The semismoothness of constitutive operators in elastoplasticity has been studied e.g. in [4, 16, 31, 35, 36, 6]. Namely in [31, 36], one can find an abstract framework how to investigate it for operators in an implicit form. However, the framework cannot be straightforwardly used for models investigated in this paper. Therefore, we introduce the following auxilliary result.

**Proposition 2.1.** Let  $p(\cdot)$ ,  $\mathbf{s}(\cdot)$ ,  $\varrho(\cdot)$ ,  $\theta(\cdot)$ ,  $\mathbf{n}(\cdot)$ ,  $r_e(\cdot)$  and  $\varrho_e(\cdot)$  be the functions introduced in Section 2.1. Further, let  $\hat{p}, \hat{\varrho} : \mathbb{R}_{sym}^{3 \times 3} \rightarrow \mathbb{R}$  be strongly semismooth functions and assume that  $\hat{\varrho}$  vanishes for any  $\boldsymbol{\sigma} \in \mathbb{R}_{sym}^{3 \times 3}$ ,  $\varrho(\boldsymbol{\sigma}) = 0$ . Define,

$$\hat{\varrho}_e(\boldsymbol{\sigma}) := \begin{cases} \hat{\varrho}(\boldsymbol{\sigma})r_e(\cos \theta(\boldsymbol{\sigma})), & \varrho(\boldsymbol{\sigma}) \neq 0, \\ 0, & \varrho(\boldsymbol{\sigma}) = 0, \end{cases}, \quad \mathbf{S}(\boldsymbol{\sigma}) := \begin{cases} \hat{p}(\boldsymbol{\sigma})\mathbf{I} + \hat{\varrho}(\boldsymbol{\sigma})\mathbf{n}(\boldsymbol{\sigma}), & \varrho(\boldsymbol{\sigma}) \neq 0, \\ \hat{p}(\boldsymbol{\sigma})\mathbf{I}, & \varrho(\boldsymbol{\sigma}) = 0. \end{cases}$$

Then the functions  $\varrho$ ,  $\varrho_e$ ,  $\hat{\varrho}_e$  and  $\mathbf{S}$  are strongly semismooth in  $\mathbb{R}_{sym}^{3 \times 3}$ .

*Proof.* Since the functions  $\mathbf{n}(\cdot)$  and  $r_e(\cos \theta(\cdot))$  are bounded and have Lipschitz continuous derivatives in  $\{\boldsymbol{\sigma} \in \mathbb{R}_{sym}^{3 \times 3} \mid \varrho(\boldsymbol{\sigma}) \neq 0\}$ , it is easy to see that the functions  $\varrho$ ,  $\varrho_e$ ,  $\hat{\varrho}_e$  and  $\mathbf{S}$  are locally Lipschitz continuous in  $\mathbb{R}_{sym}^{3 \times 3}$  and strongly semismooth for any  $\boldsymbol{\sigma} \in \mathbb{R}_{sym}^{3 \times 3}$ ,  $\varrho(\boldsymbol{\sigma}) \neq 0$ . Therefore, it remains to show strong semismoothness at  $\boldsymbol{\sigma} \in \mathbb{R}_{sym}^{3 \times 3}$ ,  $\varrho(\boldsymbol{\sigma}) = 0$ . To this end, we show that (2.9) holds for  $\varrho$ ,  $\varrho_e$ ,  $\hat{\varrho}_e$  and  $\mathbf{S}$  at such  $\boldsymbol{\sigma}$ . Let  $\boldsymbol{\tau} \in \mathbb{R}_{sym}^{3 \times 3}$  be such that  $\varrho(\boldsymbol{\tau}) \neq 0$ . Then

$$\varrho(\boldsymbol{\sigma} + \epsilon \boldsymbol{\tau}) = \epsilon \varrho(\boldsymbol{\tau}), \quad \mathbf{n}(\boldsymbol{\sigma} + \epsilon \boldsymbol{\tau}) = \mathbf{n}(\boldsymbol{\tau}), \quad \theta(\boldsymbol{\sigma} + \epsilon \boldsymbol{\tau}) = \theta(\boldsymbol{\tau}) \quad \forall \epsilon > 0.$$

Hence  $\varrho'(\boldsymbol{\sigma} + \boldsymbol{\tau}; \boldsymbol{\tau}) - \varrho'(\boldsymbol{\sigma}; \boldsymbol{\tau}) = 0$ ,  $\varrho_e'(\boldsymbol{\sigma} + \boldsymbol{\tau}; \boldsymbol{\tau}) - \varrho_e'(\boldsymbol{\sigma}; \boldsymbol{\tau}) = 0$  and

$$\begin{aligned} \hat{\varrho}_e'(\boldsymbol{\sigma} + \boldsymbol{\tau}; \boldsymbol{\tau}) - \hat{\varrho}_e'(\boldsymbol{\sigma}; \boldsymbol{\tau}) &= [\hat{\varrho}'(\boldsymbol{\sigma} + \boldsymbol{\tau}; \boldsymbol{\tau}) - \hat{\varrho}'(\boldsymbol{\sigma}; \boldsymbol{\tau})] r_e(\cos \theta(\boldsymbol{\tau})) = O(\|\boldsymbol{\tau}\|^2), \\ \mathbf{S}'(\boldsymbol{\sigma} + \boldsymbol{\tau}; \boldsymbol{\tau}) - \mathbf{S}'(\boldsymbol{\sigma}; \boldsymbol{\tau}) &= [\hat{p}'(\boldsymbol{\sigma} + \boldsymbol{\tau}; \boldsymbol{\tau}) - \hat{p}'(\boldsymbol{\sigma}; \boldsymbol{\tau})] \mathbf{I} + [\hat{\varrho}'(\boldsymbol{\sigma} + \boldsymbol{\tau}; \boldsymbol{\tau}) - \hat{\varrho}'(\boldsymbol{\sigma}; \boldsymbol{\tau})] \mathbf{n}(\boldsymbol{\tau}) = O(\|\boldsymbol{\tau}\|^2), \end{aligned}$$

since the functions  $\hat{p}$ ,  $\hat{\varrho}$  satisfy (2.9) by the assumption.  $\square$

The function  $\mathbf{S}$  introduced in Proposition 2.1 has the same scheme as a mapping between trial and unknown stress tensors for models introduced in Section 3–5. Here, the trial stress is represented by  $\boldsymbol{\sigma}$  and the unknown stress is in the form  $\hat{\boldsymbol{\sigma}} = \hat{p}(\boldsymbol{\sigma}) \mathbf{I} + \hat{\varrho}(\boldsymbol{\sigma}) \mathbf{n}(\boldsymbol{\sigma})$ . Therefore, it is sufficient to prove only semismoothness of the scalar functions  $\hat{p}$ ,  $\hat{\varrho}$  representing invariants of the unknown stress tensor. The semismoothness of  $\hat{\varrho}_e$  has been derived to prove Theorem 4.3.

## 3 The Drucker-Prager model

### 3.1 Constitutive initial value problem

We consider the elastoplastic problem containing the Drucker-Prager criterion, a nonassociative plastic flow rule and a nonlinear isotropic hardening. Within a thermodynamical framework with internal variables, we introduce the corresponding constitutive initial value problem, see [11]:

1. *Additive decomposition of the infinitesimal strain tensor  $\boldsymbol{\varepsilon}$  on elastic and plastic parts:*

$$\boldsymbol{\varepsilon} = \boldsymbol{\varepsilon}^e + \boldsymbol{\varepsilon}^p. \quad (3.1)$$

2. *Linear isotropic elastic law between the stress and the elastic strain:*

$$\boldsymbol{\sigma} = \mathbb{D}_e : \boldsymbol{\varepsilon}^e = K(\mathbf{I} : \boldsymbol{\varepsilon}^e) \mathbf{I} + 2G \mathbb{I}_{dev} : \boldsymbol{\varepsilon}^e, \quad \mathbb{D}_e = K \mathbf{I} \otimes \mathbf{I} + 2G \mathbb{I}_{dev}, \quad (3.2)$$

where  $K, G > 0$  denotes the bulk, and shear moduli, respectively.

3. *Non-linear isotropic hardening:*

$$\kappa = H(\bar{\boldsymbol{\varepsilon}}^p). \quad (3.3)$$

Here  $\bar{\boldsymbol{\varepsilon}}^p \in \mathbb{R}_+$  denotes an isotropic (scalar) hardening variable,  $\kappa \in \mathbb{R}_+$  is the corresponding thermodynamical force and  $H : \mathbb{R}_+ \rightarrow \mathbb{R}_+$  is a nondecreasing, strongly semismooth function satisfying  $H(0) = 0$ .

4. *Drucker-Prager yield function:*

$$f(\boldsymbol{\sigma}, \kappa) = \hat{f}(p(\boldsymbol{\sigma}), \varrho(\boldsymbol{\sigma}), \kappa) = \sqrt{\frac{1}{2}} \varrho + \eta p - \xi(c_0 + \kappa). \quad (3.4)$$

Here, the parameters  $\eta, \xi > 0$  are usually calculated from the friction angle using a sufficient approximation of the Mohr-Coulomb yield surface and  $c_0 > 0$  denotes the initial cohesion.

5. *Plastic pseudo-potential.*

$$g(\boldsymbol{\sigma}) = \hat{g}(p(\boldsymbol{\sigma}), \varrho(\boldsymbol{\sigma})) = \sqrt{\frac{1}{2}}\varrho + \bar{\eta}p. \quad (3.5)$$

Here  $\bar{\eta} > 0$  denotes a parameter depending on the dilatancy angle.

6. *Nonassociative plastic flow rule*

$$\dot{\boldsymbol{\varepsilon}}^p \in \dot{\lambda} \partial g(\boldsymbol{\sigma}), \quad (3.6)$$

where  $\dot{\lambda} \geq 0$  is a multiplier and  $\partial g(\boldsymbol{\sigma})$  denotes the subdifferential of the convex function  $g$  at  $\boldsymbol{\sigma}$ . Using (2.4), (2.6) and (3.5), the flow rule (3.6) can be written as

$$\dot{\boldsymbol{\varepsilon}}^p = \dot{\lambda} \left( \sqrt{\frac{1}{2}} \hat{\boldsymbol{n}} + \frac{\bar{\eta}}{3} \mathbf{I} \right), \quad \hat{\boldsymbol{n}} \in \partial \varrho(\boldsymbol{\sigma}). \quad (3.7)$$

Consequently by (3.1), (3.2) and (2.7),

$$\dot{\boldsymbol{\sigma}} = \mathbb{D}_e : (\dot{\boldsymbol{\varepsilon}} - \dot{\boldsymbol{\varepsilon}}^p) = \mathbb{D}_e : \dot{\boldsymbol{\varepsilon}} - \dot{\lambda} \left( G\sqrt{2}\hat{\boldsymbol{n}} + K\bar{\eta}\mathbf{I} \right). \quad (3.8)$$

7. *Associative hardening law:*

$$\dot{\bar{\varepsilon}}^p = -\dot{\lambda} \frac{\partial f(\boldsymbol{\sigma}, \kappa)}{\partial \kappa} = \dot{\lambda} \xi. \quad (3.9)$$

8. *Loading/unloading criterion:*

$$\dot{\lambda} \geq 0, \quad f(\boldsymbol{\sigma}, \kappa) \leq 0, \quad \dot{\lambda} f(\boldsymbol{\sigma}, \kappa) = 0. \quad (3.10)$$

Then the elastoplastic constitutive initial value problem reads as follows: *Given the history of the strain tensor  $\boldsymbol{\varepsilon} = \boldsymbol{\varepsilon}(t)$ ,  $t \in [t_0, t_{\max}]$ , and the initial values  $\boldsymbol{\varepsilon}^p(t_0) = \boldsymbol{\varepsilon}^p$ ,  $\bar{\varepsilon}^p(t_0) = \bar{\varepsilon}_0^p$ . Find  $(\boldsymbol{\sigma}(t), \boldsymbol{\varepsilon}^p(t), \bar{\varepsilon}^p(t))$  such that*

$$\left. \begin{aligned} \boldsymbol{\sigma} &= \mathbb{D}_e : (\boldsymbol{\varepsilon} - \boldsymbol{\varepsilon}^p), \\ \dot{\boldsymbol{\sigma}} &= \mathbb{D}_e : \dot{\boldsymbol{\varepsilon}} - \dot{\lambda} (G\sqrt{2}\hat{\boldsymbol{n}} + K\bar{\eta}\mathbf{I}), \quad \hat{\boldsymbol{n}} \in \partial \varrho(\boldsymbol{\sigma}), \\ \dot{\bar{\varepsilon}}^p &= \dot{\lambda} \xi, \\ \dot{\lambda} &\geq 0, \quad f(\boldsymbol{\sigma}, H(\bar{\varepsilon}^p)) \leq 0, \quad \dot{\lambda} f(\boldsymbol{\sigma}, H(\bar{\varepsilon}^p)) = 0. \end{aligned} \right\} \quad (3.11)$$

hold for each instant  $t \in [t_0, t_{\max}]$ .

### 3.2 Implicit Euler discretization of CIVP

We discretize CIVP using the implicit Euler method. To this end we assume a partition

$$0 = t_0 < t_1 < \dots < t_k < \dots < t_N = t_{\max}$$

of the pseudo-time interval and fix a step  $k$ . For the sake of brevity, we omit the index  $k$  and write  $\boldsymbol{\sigma} := \boldsymbol{\sigma}(t_k)$ ,  $\boldsymbol{\varepsilon} := \boldsymbol{\varepsilon}(t_k)$ ,  $\boldsymbol{\varepsilon}^p := \boldsymbol{\varepsilon}^p(t_k)$  and  $\bar{\varepsilon}^p = \bar{\varepsilon}^p(t_k)$ . Further, we define the following trial variables:  $\bar{\boldsymbol{\varepsilon}}^{p, tr} := \bar{\boldsymbol{\varepsilon}}^p(t_{k-1})$ ,  $\boldsymbol{\varepsilon}^{e, tr} = \boldsymbol{\varepsilon}(t_k) - \boldsymbol{\varepsilon}^p(t_{k-1})$  and  $\boldsymbol{\sigma}^{tr} := \mathbb{D}_e : \boldsymbol{\varepsilon}^{e, tr}$ . Then the discrete elastoplastic constitutive problem for the  $k$ -step reads as follows: *Given  $\boldsymbol{\varepsilon}$ ,  $\boldsymbol{\sigma}^{tr}$  and  $\bar{\boldsymbol{\varepsilon}}^{p, tr}$ . Find  $\boldsymbol{\sigma}$ ,  $\boldsymbol{\varepsilon}^p$  and  $\Delta \lambda$  satisfying:*

$$\left. \begin{aligned} \boldsymbol{\sigma} &= \boldsymbol{\sigma}^{tr} - \Delta \lambda (G\sqrt{2}\hat{\boldsymbol{n}} + K\bar{\eta}\mathbf{I}), \quad \hat{\boldsymbol{n}} \in \partial \varrho(\boldsymbol{\sigma}), \\ \bar{\varepsilon}^p &= \bar{\boldsymbol{\varepsilon}}^{p, tr} + \Delta \lambda \xi, \\ \Delta \lambda &\geq 0, \quad f(\boldsymbol{\sigma}, H(\bar{\boldsymbol{\varepsilon}}^p)) \leq 0, \quad \Delta \lambda f(\boldsymbol{\sigma}, H(\bar{\boldsymbol{\varepsilon}}^p)) = 0. \end{aligned} \right\} \quad (3.12)$$

Notice that the remaining input parameter for the next step,  $\boldsymbol{\varepsilon}^p(t_k)$ , can be computed using the formula  $\boldsymbol{\varepsilon}^p = \boldsymbol{\varepsilon} - \mathbb{D}_e^{-1} : \boldsymbol{\sigma}$  after finding a solution to problem (3.12).



### 3.3 Solution of the incremental problem

We standardly use the elastic predictor/plastic corrector method for solving (3.12).

**Elastic predictor** applies when

$$f(\boldsymbol{\sigma}^{tr}, H(\bar{\varepsilon}^{p,tr})) \leq 0. \quad (3.13)$$

Then the triplet

$$\boldsymbol{\sigma} = \boldsymbol{\sigma}^{tr}, \quad \bar{\varepsilon}^p = \bar{\varepsilon}^{p,tr}, \quad \Delta\lambda = 0 \quad (3.14)$$

is the solution to (3.12).

**Plastic corrector** applies when (3.13) does not hold. Then  $\Delta\lambda > 0$  and (3.12) reduces into

$$\left. \begin{aligned} \boldsymbol{\sigma} &= \boldsymbol{\sigma}^{tr} - \Delta\lambda (G\sqrt{2}\hat{\mathbf{n}} + K\bar{\eta}\mathbf{I}), \quad \hat{\mathbf{n}} \in \partial\varrho(\boldsymbol{\sigma}), \\ \bar{\varepsilon}^p &= \bar{\varepsilon}^{p,tr} + \Delta\lambda\xi, \\ f(\boldsymbol{\sigma}, H(\bar{\varepsilon}^p)) &= 0. \end{aligned} \right\} \quad (3.15)$$

Since the functions  $f$  and  $g$  depend on  $\boldsymbol{\sigma}$  only through the variables  $\varrho$  and  $p$ , it is natural to reduce a number of unknowns in problem (3.15). To this end, we split (3.15)<sub>1</sub> into the deviatoric and volumetric parts:

$$\mathbf{s} = \mathbf{s}^{tr} - \Delta\lambda G\sqrt{2}\hat{\mathbf{n}}, \quad \hat{\mathbf{n}} \in \partial\varrho(\boldsymbol{\sigma}), \quad (3.16)$$

$$p = p^{tr} - \Delta\lambda K\bar{\eta}, \quad (3.17)$$

where  $\mathbf{s}^{tr}$ ,  $p^{tr}$  denotes the deviatoric stress, and the hydrostatic stress related to  $\boldsymbol{\sigma}^{tr}$ , respectively. Using (2.4)<sub>3</sub>, the equality (3.16) yields

$$\mathbf{s}^{tr} = \begin{cases} \left(1 + \frac{\Delta\lambda G\sqrt{2}}{\varrho}\right) \mathbf{s} & \text{if } \varrho > 0, \\ \Delta\lambda G\sqrt{2}\hat{\mathbf{n}} & \text{if } \varrho = 0. \end{cases} \quad (3.18)$$

Denote  $\varrho^{tr} = \|\mathbf{s}^{tr}\|$  and recall that  $\|\hat{\mathbf{n}}\| \leq 1$  for  $\varrho = 0$  by (2.6). Then from (3.18) we obtain

$$\begin{cases} \varrho = \varrho^{tr} - \Delta\lambda G\sqrt{2} & \text{if } \varrho > 0, \\ 0 \geq \varrho^{tr} - \Delta\lambda G\sqrt{2} & \text{if } \varrho = 0. \end{cases} \quad (3.19)$$

Following the arguments developed in Section 1.1, we now rewrite (3.19) as follows:

$$\varrho = \left(\varrho^{tr} - \Delta\lambda G\sqrt{2}\right)^+ = \max\left\{0; \varrho^{tr} - \Delta\lambda G\sqrt{2}\right\}. \quad (3.20)$$

Notice that (3.19) and (3.20) are equivalent. Further from (3.18)<sub>1</sub>, we standardly have:

$$\mathbf{n} = \frac{\mathbf{s}}{\varrho} = \frac{\mathbf{s}^{tr}}{\varrho^{tr}} = \mathbf{n}^{tr} \quad \text{if } \varrho > 0. \quad (3.21)$$

The following theorem summarizes and completes the derived results.

**Theorem 3.1.** *Let  $f(\boldsymbol{\sigma}^{tr}, H(\bar{\varepsilon}^{p,tr})) > 0$ . If  $(\boldsymbol{\sigma}, \bar{\varepsilon}^p, \Delta\lambda)$  is a solution to problem (3.15) and  $p = \mathbf{I} : \boldsymbol{\sigma}/3$ ,  $\mathbf{s} = \mathbb{I}_{dev} : \boldsymbol{\sigma}$ ,  $\varrho = \|\mathbf{s}\|$ , then  $(p, \varrho, \bar{\varepsilon}^p, \Delta\lambda)$  is a solution to the following system:*

$$\left. \begin{aligned} p &= p^{tr} - \Delta\lambda K\bar{\eta}, \\ \varrho &= \left(\varrho^{tr} - \Delta\lambda G\sqrt{2}\right)^+, \\ \bar{\varepsilon}^p &= \bar{\varepsilon}^{p,tr} + \Delta\lambda\xi, \\ \hat{f}(p, \varrho, H(\bar{\varepsilon}^p)) &= 0. \end{aligned} \right\} \quad (3.22)$$

Conversely, if  $(p, \varrho, \bar{\varepsilon}^p, \Delta\lambda)$  is a solution to (3.22) then  $(\boldsymbol{\sigma}, \bar{\varepsilon}^p, \Delta\lambda)$  is the solution to (3.15) where

$$\boldsymbol{\sigma} = \begin{cases} \boldsymbol{\sigma}^{tr} - \Delta\lambda (G\sqrt{2}\mathbf{n}^{tr} + K\bar{\eta}\mathbf{I}) & \text{if } \varrho^{tr} > \Delta\lambda G\sqrt{2}, \\ (p^{tr} - \Delta\lambda K\bar{\eta})\mathbf{I} & \text{if } \varrho^{tr} \leq \Delta\lambda G\sqrt{2}. \end{cases} \quad (3.23)$$

Notice that the knowledge of the subdifferential of  $\varrho$  enables us to formulate the plastic corrector problem as a unique system of nonlinear equations in comparison to the current technique introduced in [11]. Moreover, one can eliminate the unknowns  $p, \varrho, \bar{\varepsilon}^p$  similarly as for the current return-mapping scheme of this model. Inserting of (3.22)<sub>1-3</sub> into (3.22)<sub>4</sub> leads to the nonlinear equation  $q_{tr}(\Delta\lambda) = 0$  where

$$q_{tr}(\gamma) := q(\gamma; p^{tr}, \varrho^{tr}, \bar{\varepsilon}^{p, tr}) = \sqrt{\frac{1}{2}} \left( \varrho^{tr} - \gamma G \sqrt{2} \right)^+ + \eta(p^{tr} - \gamma K \bar{\eta}) - \xi(c_0 + H(\bar{\varepsilon}^{p, tr} + \gamma \xi)), \quad \gamma \in \mathbb{R}_+, \quad (3.24)$$

using (3.4). We have the following solvability result.

**Theorem 3.2.** *Let  $f(\boldsymbol{\sigma}^{tr}, H(\bar{\varepsilon}^{p, tr})) > 0$ . Then there exists a unique solution,  $\Delta\lambda > 0$ , of the equation  $q_{tr}(\Delta\lambda) = 0$ . Furthermore, problems (3.22), (3.15) and (3.12) have also unique solutions.*

*In addition, if  $q_{tr}(\varrho^{tr}/G\sqrt{2}) < 0$  then  $\Delta\lambda \in (0, \varrho^{tr}/G\sqrt{2})$  and  $\varrho > 0$ . Conversely, if  $q_{tr}(\varrho^{tr}/G\sqrt{2}) \geq 0$  then  $\Delta\lambda \geq \varrho^{tr}/G\sqrt{2}$  and  $\varrho = 0$ .*

*Proof.* From (3.24) and the assumptions on  $H$ , it is readily seen that  $q_{tr}$  is a continuous and decreasing function. Further,  $q_{tr}(\gamma) \rightarrow -\infty$  as  $\gamma \rightarrow +\infty$  and  $q_{tr}(0) = f(\boldsymbol{\sigma}^{tr}, H(\bar{\varepsilon}^{p, tr})) > 0$ . Therefore, the equation  $q_{tr}(\Delta\lambda) = 0$  has just one solution in  $\mathbb{R}_+$ . If  $q_{tr}(\varrho^{tr}/G\sqrt{2}) < 0$  then  $\Delta\lambda \in (0, \varrho^{tr}/G\sqrt{2})$ . Otherwise,  $\Delta\lambda \geq \varrho^{tr}/G\sqrt{2}$ . The rest of the proof follows from Theorem 3.1 and the elastic prediction.  $\square$

The second part of Theorem 3.2 is very useful from the computational point of view: one can a priori decide whether return to the smooth portion of the yield surface happens or not. This is the main difference in comparison with the current return-mapping scheme. The improved return-mapping scheme reads as follows.

### Return to the smooth portion

1. *Necessary and sufficient condition:*  $q_{tr}(0) > 0$  and  $q_{tr}(\varrho^{tr}/G\sqrt{2}) < 0$ .
2. *Find  $\Delta\lambda \in (0, \varrho^{tr}/G\sqrt{2})$ :*

$$\sqrt{\frac{1}{2}} \left( \varrho^{tr} - \Delta\lambda G \sqrt{2} \right) + \eta(p^{tr} - \Delta\lambda K \bar{\eta}) - \xi(c_0 + H(\bar{\varepsilon}^{p, tr} + \Delta\lambda \xi)) = 0. \quad (3.25)$$

3. *Set*

$$\boldsymbol{\sigma} = \boldsymbol{\sigma}^{tr} - \Delta\lambda \left( G\sqrt{2} \mathbf{n}^{tr} + K \bar{\eta} \mathbf{I} \right), \quad \bar{\varepsilon}^p = \bar{\varepsilon}^{p, tr} + \Delta\lambda \xi. \quad (3.26)$$

### Return to the apex

1. *Necessary and sufficient condition:*  $q_{tr}(\varrho^{tr}/G\sqrt{2}) \geq 0$ .
2. *Find  $\Delta\lambda \geq \varrho^{tr}/G\sqrt{2}$ :*

$$\eta(p^{tr} - \Delta\lambda K \bar{\eta}) - \xi(c_0 + H(\bar{\varepsilon}^{p, tr} + \Delta\lambda \xi)) = 0. \quad (3.27)$$

3. *Set*

$$\boldsymbol{\sigma} = (p^{tr} - \Delta\lambda K \bar{\eta}) \mathbf{I}, \quad \bar{\varepsilon}^p = \bar{\varepsilon}^{p, tr} + \Delta\lambda \xi. \quad (3.28)$$

Nonlinear equations (3.25) and (3.27) can be solved by the Newton method. Then it is natural to use the initial choice  $\Delta\lambda^0 = 0$ ,  $\Delta\lambda^0 = \varrho^{tr}/G\sqrt{2}$  for (3.25), and (3.27), respectively. In case of perfect plasticity,  $H = 0$ , or linear hardening,  $H(\bar{\varepsilon}^p) = \tilde{H} \bar{\varepsilon}^p$ ,  $\tilde{H} = \text{const.}$ , equations (3.25) and (3.27) are linear and thus  $\Delta\lambda$  can be found in the closed form.

### 3.4 Stress-strain and consistent tangent operators

Solving the problem (3.12), we obtain a nonlinear and implicit operator between the stress tensor,  $\boldsymbol{\sigma} = \boldsymbol{\sigma}(t_k)$ , and the strain tensor,  $\boldsymbol{\varepsilon} = \boldsymbol{\varepsilon}(t_k)$ . The stress-strain operator,  $\mathbf{T}$ , also depends on  $\boldsymbol{\varepsilon}^p(t_{k-1})$  and  $\bar{\boldsymbol{\varepsilon}}^p(t_{k-1})$  through the trial variables. To emphasize this fact we write  $\boldsymbol{\sigma} := \mathbf{T}(\boldsymbol{\varepsilon}; \boldsymbol{\varepsilon}^p(t_{k-1}), \bar{\boldsymbol{\varepsilon}}^p(t_{k-1}))$ . From the results introduced in Section 3.3, we have  $\mathbf{T}(\boldsymbol{\varepsilon}; \boldsymbol{\varepsilon}^p(t_{k-1}), \bar{\boldsymbol{\varepsilon}}^p(t_{k-1})) = \mathbf{S}(\boldsymbol{\sigma}^{tr}, \bar{\boldsymbol{\varepsilon}}^{p,tr})$ , where

$$\mathbf{S}(\boldsymbol{\sigma}^{tr}, \bar{\boldsymbol{\varepsilon}}^{p,tr}) = \begin{cases} \boldsymbol{\sigma}^{tr} & \text{if } q_{tr}(0) \leq 0, \\ \boldsymbol{\sigma}^{tr} - \Delta\lambda (G\sqrt{2}\mathbf{n}^{tr} + K\bar{\eta}\mathbf{I}) & \text{if } q_{tr}(0) > 0, q_{tr}(\varrho^{tr}/G\sqrt{2}) < 0, \\ (p^{tr} - \Delta\lambda K\bar{\eta})\mathbf{I} & \text{if } q_{tr}(\varrho^{tr}/G\sqrt{2}) \geq 0, \end{cases} \quad (3.29)$$

where  $\Delta\lambda$  is the solution to (3.25), (3.27) in (3.29)<sub>2</sub>, and (3.29)<sub>3</sub>, respectively, i.e.  $q_{tr}(\Delta\lambda) = 0$ .

**Theorem 3.3.** *The function  $\mathbf{T}$  is strongly semismooth in  $\mathbb{R}_{sym}^{3 \times 3}$  with respect to  $\boldsymbol{\varepsilon}$ .*

*Proof.* We use the framework introduced in Section 2.2. Consider the function  $\Delta\lambda := \Delta\lambda(\boldsymbol{\sigma}^{tr}, \bar{\boldsymbol{\varepsilon}}^{p,tr})$  satisfying  $\Delta\lambda = 0$  if  $q_{tr}(0) \leq 0$ , otherwise  $q_{tr}(\Delta\lambda) = 0$ . Applying Theorem 2.1 on the implicit function  $q_{tr}$ , one can easily find that the function  $\Delta\lambda$  is strongly semismooth. Consequently, the functions  $\hat{p}(\boldsymbol{\sigma}^{tr}, \bar{\boldsymbol{\varepsilon}}^{p,tr}) = p^{tr} - (\Delta\lambda)^+ K\bar{\eta}$  and  $\hat{\varrho}(\boldsymbol{\sigma}^{tr}, \bar{\boldsymbol{\varepsilon}}^{p,tr}) = (\varrho^{tr} - (\Delta\lambda)^+ G\sqrt{2})^+$  are strongly semismooth. Since  $\mathbf{S}(\boldsymbol{\sigma}^{tr}, \bar{\boldsymbol{\varepsilon}}^{p,tr}) = \hat{p}(\boldsymbol{\sigma}^{tr}, \bar{\boldsymbol{\varepsilon}}^{p,tr})\mathbf{I} + \hat{\varrho}(\boldsymbol{\sigma}^{tr}, \bar{\boldsymbol{\varepsilon}}^{p,tr})\mathbf{n}(\boldsymbol{\sigma}^{tr})$ , we obtain strong semismoothness of the functions  $\mathbf{S}$  and  $\mathbf{T}$  using Proposition 2.1.  $\square$

Notice that  $\mathbf{T}$  is not smooth if  $q_{tr}(0) = 0$  or  $q_{tr}(\varrho^{tr}/G\sqrt{2}) = 0$  or if  $H$  has not derivative at  $\bar{\boldsymbol{\varepsilon}}^{p,tr} + \Delta\lambda\xi$ . We introduce the derivative  $\partial\boldsymbol{\sigma}/\partial\boldsymbol{\varepsilon}$  under the assumption that any of these conditions does not hold. Set  $H_1 := H'(\bar{\boldsymbol{\varepsilon}}^{p,tr} + \Delta\lambda\xi)$ . Using (2.4), (2.5), (3.2) and the chain rule, we obtain the following auxilliary derivatives:

$$\frac{\partial\boldsymbol{\sigma}^{tr}}{\partial\boldsymbol{\varepsilon}} = \mathbb{D}_e, \quad \frac{\partial p^{tr}}{\partial\boldsymbol{\varepsilon}} = K\mathbf{I}, \quad \frac{\partial s^{tr}}{\partial\boldsymbol{\varepsilon}} = 2G\mathbb{I}_{dev}, \quad \frac{\partial\varrho^{tr}}{\partial\boldsymbol{\varepsilon}} = 2G\mathbf{n}^{tr}, \quad \frac{\partial\mathbf{n}^{tr}}{\partial\boldsymbol{\varepsilon}} = \frac{2G}{\varrho^{tr}} (\mathbb{I}_{dev} - \mathbf{n}^{tr} \otimes \mathbf{n}^{tr}).$$

We distinguish three possible cases:

1. Let  $q_{tr}(0) < 0$  (*elastic response*). Then clearly,

$$\frac{\partial\boldsymbol{\sigma}}{\partial\boldsymbol{\varepsilon}} = \mathbb{D}_e. \quad (3.30)$$

2. Let  $q_{tr}(0) > 0$  and  $q_{tr}(\varrho^{tr}/G\sqrt{2}) < 0$  (*return to the smooth surface*). Then the derivative of (3.26) reads

$$\frac{\partial\boldsymbol{\sigma}}{\partial\boldsymbol{\varepsilon}} = \mathbb{D}_e - \Delta\lambda \frac{2G^2\sqrt{2}}{\varrho^{tr}} (\mathbb{I}_{dev} - \mathbf{n}^{tr} \otimes \mathbf{n}^{tr}) - (G\sqrt{2}\mathbf{n}^{tr} + K\bar{\eta}\mathbf{I}) \otimes \frac{\partial\Delta\lambda}{\partial\boldsymbol{\varepsilon}}.$$

Applying the implicit function theorem on (3.25), we obtain

$$\frac{\partial\Delta\lambda}{\partial\boldsymbol{\varepsilon}} = \frac{G\sqrt{2}\mathbf{n}^{tr} + \eta K\mathbf{I}}{G + K\eta\bar{\eta} + \xi^2 H_1}.$$

Hence,

$$\frac{\partial\boldsymbol{\sigma}}{\partial\boldsymbol{\varepsilon}} = \mathbb{D}_e - \Delta\lambda \frac{2G^2\sqrt{2}}{\varrho^{tr}} (\mathbb{I}_{dev} - \mathbf{n}^{tr} \otimes \mathbf{n}^{tr}) - (G\sqrt{2}\mathbf{n}^{tr} + K\bar{\eta}\mathbf{I}) \otimes \frac{G\sqrt{2}\mathbf{n}^{tr} + \eta K\mathbf{I}}{G + K\eta\bar{\eta} + \xi^2 H_1}. \quad (3.31)$$

3. Let  $q_{tr}(\varrho^{tr}/G\sqrt{2}) > 0$  (return to the apex). Then the derivative of (3.28) yields

$$\frac{\partial \boldsymbol{\sigma}}{\partial \boldsymbol{\varepsilon}} = K \left( \mathbf{I} \otimes \mathbf{I} - \bar{\eta} \mathbf{I} \otimes \frac{\partial \Delta \lambda}{\partial \boldsymbol{\varepsilon}} \right).$$

Applying the implicit function theorem on (3.27), we obtain

$$\frac{\partial \Delta \lambda}{\partial \boldsymbol{\varepsilon}} = \frac{\eta K}{K \eta \bar{\eta} + \xi^2 H_1} \mathbf{I}.$$

Hence,

$$\frac{\partial \boldsymbol{\sigma}}{\partial \boldsymbol{\varepsilon}} = K \left( 1 - \frac{K \eta \bar{\eta}}{K \eta \bar{\eta} + \xi^2 H_1} \right) \mathbf{I} \otimes \mathbf{I}. \quad (3.32)$$

The derivatives (3.30)–(3.32) define the consistent tangent operator,  $\mathbb{T}^\circ$ . It is readily seen that the tangent operator is symmetric if  $\bar{\eta} = \eta$ , i.e. for the associative plasticity. For purposes of Section 6, it is useful to extend the definition of  $\mathbb{T}^\circ$  for nondifferential points. For example, one can write

$$\mathbb{T}^\circ(\boldsymbol{\varepsilon}; \boldsymbol{\varepsilon}^p(t_{k-1}), \bar{\boldsymbol{\varepsilon}}^p(t_{k-1})) = \begin{cases} \mathbb{D}_e & \text{if } q_{tr}(0) \leq 0, \\ (3.31) & \text{if } q_{tr}(0) > 0, q_{tr}(\varrho^{tr}/G\sqrt{2}) < 0, \\ (3.32) & \text{if } q_{tr}(\varrho^{tr}/G\sqrt{2}) \geq 0, \end{cases} \quad (3.33)$$

where  $H_1$  in (3.31), (3.32) is the derivative from left of  $H$  at  $\bar{\boldsymbol{\varepsilon}}^{p,tr} + \Delta \lambda \boldsymbol{\xi}$ . Notice that

$$\mathbb{T}^\circ(\boldsymbol{\varepsilon}; \boldsymbol{\varepsilon}^p(t_{k-1}), \bar{\boldsymbol{\varepsilon}}^p(t_{k-1})) \in \partial_{\boldsymbol{\varepsilon}} \mathbf{T}(\boldsymbol{\varepsilon}; \boldsymbol{\varepsilon}^p(t_{k-1}), \bar{\boldsymbol{\varepsilon}}^p(t_{k-1})).$$

## 4 A simplified version of the Jirásek-Grassl model

The Jirásek-Grassl model was introduced in [15]. It is a plastic-damage model proposed for complex modelling of concrete failure. The model has been further developed. For example, Unteregger and Hofstetter [38] have improved a hardening law and used the model in rock mechanics. For the sake of simplicity, we only consider a perfect plastic part of this model to illustrate the suggested idea and improve the implicit return-mapping scheme. The whole plastic part of the Jirásek-Grassl model can be included to an abstract model studied in the next section.

### 4.1 Constitutive problem and its solution

The perfect plastic model contains the yield function proposed in [22]:

$$f(\boldsymbol{\sigma}) = \hat{f}(p(\boldsymbol{\sigma}), \varrho(\boldsymbol{\sigma}), \varrho_e(\boldsymbol{\sigma})) = \frac{3}{2} \left( \frac{\varrho}{\bar{f}_c} \right)^2 + m_0 \left( \frac{\varrho_e}{\sqrt{6}\bar{f}_c} + \frac{p}{\bar{f}_c} \right) - 1, \quad (4.1)$$

where  $m_0$  is the friction parameter and  $\bar{f}_c$  is the uniaxial compressive strength. The invariants  $p$ ,  $\varrho$  and  $\varrho_e = \varrho r_e(\cos \theta)$  were introduced in Section 2. Notice that the couple  $(p^a, \varrho^a) = (\bar{f}_c/m_0, 0)$  defines the apex of the yields surface generated by the function  $\hat{f}$ . The yield surface is not smooth only at this apex. Scheme of the yield surface can be found in [15].

Further, the following plastic pseudo-potential is considered [15]:

$$g(\boldsymbol{\sigma}) = \hat{g}(p(\boldsymbol{\sigma}), \varrho(\boldsymbol{\sigma})) = \frac{3}{2} \left( \frac{\varrho}{\bar{f}_c} \right)^2 + \frac{m_0 \varrho}{\sqrt{6}\bar{f}_c} + \frac{m_g(p)}{\bar{f}_c}, \quad (4.2)$$

where

$$m_g(p) = A_g B_g \bar{f}_c e^{\frac{p - \bar{f}_t/3}{B_g \bar{f}_c}}, \quad A_g, B_g, \bar{f}_c, \bar{f}_t > 0. \quad (4.3)$$

The subdifferential of  $g$  consists of the following directions:

$$\frac{1}{3}\hat{g}_V(p(\boldsymbol{\sigma}), \varrho(\boldsymbol{\sigma}))\mathbf{I} + \hat{g}_\varrho(p(\boldsymbol{\sigma}), \varrho(\boldsymbol{\sigma}))\hat{\mathbf{n}}, \quad \hat{\mathbf{n}} \in \partial\varrho(\boldsymbol{\sigma}),$$

where  $\partial\varrho(\boldsymbol{\sigma})$  is defined by (2.6) and

$$\hat{g}_V(p, \varrho) := \frac{\partial\hat{g}}{\partial p} = \frac{m'_g(p)}{f_c}, \quad \hat{g}_\varrho(p, \varrho) := \frac{\partial\hat{g}}{\partial\varrho} = \frac{3\varrho}{f_c^2} + \frac{m_0}{\sqrt{6}f_c}, \quad m'_g(p) = A_g e^{\frac{p-\hat{f}_t/3}{B_g f_c}}.$$

The  $k$ -step of the incremental constitutive problem received by the implicit Euler method reads as follows. *Given  $\boldsymbol{\varepsilon} := \boldsymbol{\varepsilon}(t_k)$  and  $\boldsymbol{\sigma}^{tr} := \mathbb{D}_e : (\boldsymbol{\varepsilon}(t_k) - \boldsymbol{\varepsilon}^p(t_{k-1}))$ . Find  $\boldsymbol{\sigma} = \boldsymbol{\sigma}(t_k)$  and  $\Delta\lambda$  satisfying:*

$$\left. \begin{aligned} \boldsymbol{\sigma} &= \boldsymbol{\sigma}^{tr} - \Delta\lambda \left[ K \frac{m'_g(p)}{f_c} \mathbf{I} + 2G \left( \frac{3\varrho}{f_c^2} + \frac{m_0}{\sqrt{6}f_c} \right) \hat{\mathbf{n}} \right], \quad \hat{\mathbf{n}} \in \partial\varrho(\boldsymbol{\sigma}), \\ \Delta\lambda &\geq 0, \quad \hat{f}(p(\boldsymbol{\sigma}), \varrho(\boldsymbol{\sigma}), \varrho_e(\boldsymbol{\sigma})) \leq 0, \quad \Delta\lambda \hat{f}(p(\boldsymbol{\sigma}), \varrho(\boldsymbol{\sigma}), \varrho_e(\boldsymbol{\sigma})) = 0. \end{aligned} \right\} \quad (4.4)$$

We solve this problem again by the elastic predictor/plastic corrector method. Within the plastic correction, we define the trial variables  $\mathbf{s}^{tr}$ ,  $p^{tr}$ ,  $\varrho^{tr}$ ,  $\mathbf{n}^{tr} = \mathbf{s}^{tr}/\varrho^{tr}$ ,  $\theta^{tr}$ ,  $r_e^{tr} = r_e(\cos\theta^{tr})$  and  $\varrho_e^{tr}$  associated with  $\boldsymbol{\sigma}^{tr}$  and obtain the following result.

**Theorem 4.1.** *Let  $\hat{f}(p^{tr}, \varrho^{tr}, \varrho_e^{tr}) > 0$ . If  $(\boldsymbol{\sigma}, \Delta\lambda)$  is a solution to problem (4.4) and  $p = \mathbf{I} : \boldsymbol{\sigma}/3$ ,  $\mathbf{s} = \mathbb{I}_{dev} : \boldsymbol{\sigma}$ ,  $\varrho = \|\mathbf{s}\|$ , then  $(p, \varrho, \Delta\lambda)$  is a solution to the following system:*

$$\left. \begin{aligned} p &= p^{tr} - \Delta\lambda K \frac{m'_g(p)}{f_c}, \\ \varrho &= \left[ \varrho^{tr} - \Delta\lambda 2G \left( \frac{3\varrho}{f_c^2} + \frac{m_0}{\sqrt{6}f_c} \right) \right]^+, \\ \hat{f}(p, \varrho, \varrho_e^{tr}) &= 0. \end{aligned} \right\} \quad (4.5)$$

Conversely, if  $(p, \varrho, \Delta\lambda)$  is a solution to (4.5) then  $(\boldsymbol{\sigma}, \Delta\lambda)$  is the solution to (4.4) where

$$\boldsymbol{\sigma} = \begin{cases} p\mathbf{I} + \varrho\mathbf{n}^{tr} & \text{if } \varrho^{tr} > \Delta\lambda 2G \left( \frac{3\varrho}{f_c^2} + \frac{m_0}{\sqrt{6}f_c} \right), \\ p\mathbf{I} & \text{if } \varrho^{tr} \leq \Delta\lambda 2G \left( \frac{3\varrho}{f_c^2} + \frac{m_0}{\sqrt{6}f_c} \right). \end{cases} \quad (4.6)$$

*Proof.* To prove Theorem 4.1 we use the same technique as in Section 3.3. It is based on the splitting the stress tensor on the deviatoric and volumetric parts, and on using linear dependence between  $\mathbf{s}$  and  $\mathbf{s}^{tr}$  to reduce a number of unknowns. In particular, we have

$$\mathbf{s}^{tr} = \left( 1 + \Delta\lambda 2G \left( \frac{3\varrho}{f_c^2} + \frac{m_0}{\sqrt{6}f_c} \right) \frac{1}{\varrho} \right) \mathbf{s}$$

for  $\varrho > 0$ . Consequently, we obtain (4.5)<sub>2</sub>,  $\mathbf{n} = \mathbf{n}^{tr}$  and also  $\theta = \theta^{tr}$  for  $\varrho > 0$  using (2.1). Finally, notice that  $\varrho_e^{tr} \rightarrow 0$  as  $\varrho^{tr} \rightarrow 0_+$ . Indeed,  $\varrho \rightarrow 0$  as  $\varrho^{tr} \rightarrow 0_+$  and the function  $r_e(\cos(\cdot))$  is bounded.  $\square$

Analogously to the Drucker-Prager model, one can analyze existence and uniqueness of a solution to problem (4.5), and a priori decide whether the return to the smooth portion of the yield surface happens or not. To this end, we define implicit functions  $\hat{p}_{tr} : \gamma \mapsto p_\gamma$  and  $\hat{\varrho}_{tr} : \gamma \mapsto \varrho_\gamma$  such that

$$p_\gamma + \gamma K \frac{m'_g(p_\gamma)}{f_c} - p^{tr} = 0, \quad \varrho_\gamma - \left[ \varrho^{tr} - \gamma 2G \left( \frac{3\varrho_\gamma}{f_c^2} + \frac{m_0}{\sqrt{6}f_c} \right) \right]^+ = 0,$$

respectively, for any  $\gamma \geq 0$ . The following lemma is a consequence of the implicit function theorem.

**Lemma 4.1.** *The functions  $\hat{p}_{tr}$  and  $\hat{q}_{tr}$  are well-defined in  $\mathbb{R}_+$ . Further,  $\hat{p}_{tr}$  is smooth and decreasing in  $\mathbb{R}_+$ ,  $\hat{q}_{tr}$  is decreasing in the interval  $\left[0, \frac{\sqrt{6}\bar{f}_c\varrho^{tr}}{2Gm_0}\right)$  and its closed form reads as follows:*

$$\hat{q}_{tr}(\gamma) = \frac{1}{1 + \gamma \frac{6G}{f_c^2}} \left( \varrho^{tr} - \gamma \frac{2Gm_0}{\sqrt{6}\bar{f}_c} \right)^+ \quad \forall \gamma \geq 0. \quad (4.7)$$

Now, consider the function  $q_{tr}(\gamma) := q(\gamma; p^{tr}, \varrho^{tr})$ ,

$$q_{tr}(\gamma) = \hat{f}(\hat{p}_{tr}(\gamma), \hat{q}_{tr}(\gamma), \hat{q}_{tr}(\gamma)r_e^{tr}) = \frac{3}{2} \left( \frac{\hat{q}_{tr}(\gamma)}{\bar{f}_c} \right)^2 + m_0 \left( \frac{\hat{q}_{tr}(\gamma)r_e^{tr}}{\sqrt{6}\bar{f}_c} + \frac{\hat{p}_{tr}(\gamma)}{\bar{f}_c} \right) - 1. \quad (4.8)$$

**Theorem 4.2.** *Let  $\hat{f}(p^{tr}, \varrho^{tr}, \varrho_e^{tr}) > 0$ . Then there exists a unique solution,  $\Delta\lambda > 0$ , of the equation  $q_{tr}(\Delta\lambda) = 0$ . Furthermore, problems (4.5) and (4.4) have also unique solutions.*

*In addition, if  $q_{tr}(\sqrt{6}\bar{f}_c\varrho^{tr}/2Gm_0) < 0$  then  $\Delta\lambda \in (0, \sqrt{6}\bar{f}_c\varrho^{tr}/2Gm_0)$  and  $\varrho > 0$ . Conversely, if  $q_{tr}(\sqrt{6}\bar{f}_c\varrho^{tr}/2Gm_0) \geq 0$  then  $\Delta\lambda \geq \sqrt{6}\bar{f}_c\varrho^{tr}/2Gm_0$  and  $\varrho = 0$ .*

*Proof.* Since  $\hat{q}_{tr} > 0$  and  $\hat{q}'_{tr} < 0$  in  $\left[0, \frac{\sqrt{6}\bar{f}_c\varrho^{tr}}{2Gm_0}\right)$ , the functions  $\hat{q}_{tr}, \hat{q}_{tr}^2$  are decreasing in this interval. For  $\gamma \geq \frac{\sqrt{6}\bar{f}_c\varrho^{tr}}{2Gm_0}$ , these functions vanish. Therefore, from (4.8) and Lemma 4.1, it follows that  $q_{tr}$  is a continuous and decreasing function in  $\mathbb{R}_+$ . Furthermore,  $q_{tr}(\gamma) \rightarrow -\infty$  as  $\gamma \rightarrow +\infty$  and  $q(0) = \hat{f}(p^{tr}, \varrho^{tr}, \varrho_e^{tr}) > 0$ . Hence, the equation  $q_{tr}(\Delta\lambda) = 0$  has a unique solution in  $\mathbb{R}_+$ . If  $q_{tr}(\sqrt{6}\bar{f}_c\varrho^{tr}/2Gm_0) < 0$  then  $\Delta\lambda \in (0, \sqrt{6}\bar{f}_c\varrho^{tr}/2Gm_0)$ . Otherwise,  $\Delta\lambda \geq \sqrt{6}\bar{f}_c\varrho^{tr}/2Gm_0$ . The rest of the proof follows from Theorem 4.1 and the elastic prediction.  $\square$

Although the function  $q_{tr}$  is implicit the decision criterion introduced in Theorem 4.2 can be found in closed form.

**Lemma 4.2.**

$$q_{tr} \left( \frac{\sqrt{6}\bar{f}_c\varrho^{tr}}{2Gm_0} \right) \geq 0 \quad \text{if and only if} \quad p^{tr} - \frac{\sqrt{6}K}{2G} \frac{m'_g(p^a)}{m_0} \varrho^{tr} - p^a \geq 0, \quad p^a = \frac{\bar{f}_c}{m_0}. \quad (4.9)$$

*Proof.* Since  $\hat{q}_{tr} \left( \frac{\sqrt{6}\bar{f}_c\varrho^{tr}}{2Gm_0} \right) = 0$ ,

$$q_{tr} \left( \frac{\sqrt{6}\bar{f}_c\varrho^{tr}}{2Gm_0} \right) \stackrel{(4.8)}{=} \frac{m_0}{\bar{f}_c} \hat{p}_{tr} \left( \frac{\sqrt{6}\bar{f}_c\varrho^{tr}}{2Gm_0} \right) - 1 \geq 0.$$

Hence,  $p^{crit} := \hat{p}_{tr} \left( \frac{\sqrt{6}\bar{f}_c\varrho^{tr}}{2Gm_0} \right) \geq p^a$ . Using the definitions of  $\hat{p}_{tr}$  and  $m_g$ , we have

$$0 = p^{crit} - \frac{\sqrt{6}\varrho^{tr}}{2Gm_0} K m'_g(p^{crit}) - p^{tr} \geq p^a - \frac{\sqrt{6}\varrho^{tr}}{2Gm_0} K m'_g(p^a) - p^{tr}.$$

$\square$

By Theorem 4.1 and Theorem 4.2, the return-mapping scheme reads as follows.

### Return to the smooth portion

1. *Necessary and sufficient condition:*  $q_{tr}(0) > 0$  and  $q_{tr}(\sqrt{6}\bar{f}_c\varrho^{tr}/2Gm_0) < 0$ .

2. Find  $p \in \mathbb{R}$ ,  $\varrho > 0$  and  $\Delta\lambda \in (0, \sqrt{6}\bar{f}_c\varrho^{tr}/2Gm_0)$ :

$$\left. \begin{aligned} p + \Delta\lambda K \frac{m'_g(p)}{f_c} - p^{tr} &= 0, \\ \varrho + \Delta\lambda 2G \left( \frac{3\varrho}{f_c^2} + \frac{m_0}{\sqrt{6}\bar{f}_c} \right) - \varrho^{tr} &= 0, \\ \frac{3}{2} \left( \frac{\varrho}{f_c} \right)^2 + m_0 \left( \frac{\varrho r_e^{tr}}{\sqrt{6}\bar{f}_c} + \frac{p}{f_c} \right) - 1 &= 0. \end{aligned} \right\} \quad (4.10)$$

3. Set

$$\boldsymbol{\sigma} = p\mathbf{I} + \varrho\mathbf{n}^{tr}. \quad (4.11)$$

### Return to the apex

1. Necessary and sufficient condition:  $q_{tr}(\sqrt{6}\bar{f}_c\varrho^{tr}/2Gm_0) \geq 0$ .

2. Set

$$p = \frac{\bar{f}_c}{m_0}, \quad \varrho = 0, \quad \boldsymbol{\sigma} = p\mathbf{I}, \quad \Delta\lambda = \frac{\bar{f}_c}{Km'_g(p)}(p^{tr} - p). \quad (4.12)$$

The system (4.10) of nonlinear equations can be solved by the Newton method with the initial choice  $p^0 = p^{tr}$ ,  $\varrho^0 = \varrho^{tr}$ ,  $\Delta\lambda^0 = 0$ . It was shown that the system has a unique solution subject to  $q_{tr}(0) > 0$  and  $q_{tr}(\sqrt{6}\bar{f}_c\varrho^{tr}/2Gm_0) < 0$ . Without these conditions, one cannot guarantee existence and uniqueness of the solution to (4.10).

## 4.2 Stress-strain and consistent tangent operators

Solving the problem (4.4), we obtain a nonlinear and implicit operator between the stress tensor,  $\boldsymbol{\sigma} = \boldsymbol{\sigma}(t_k)$ , and the strain tensor,  $\boldsymbol{\varepsilon} = \boldsymbol{\varepsilon}(t_k)$ . The stress-strain operator,  $\mathbf{T}$ , also depends on  $\boldsymbol{\varepsilon}^p(t_{k-1})$  through the trial stress. To emphasize this fact we write  $\boldsymbol{\sigma} := \mathbf{T}(\boldsymbol{\varepsilon}; \boldsymbol{\varepsilon}^p(t_{k-1}))$ . We have

$$\mathbf{T}(\boldsymbol{\varepsilon}; \boldsymbol{\varepsilon}^p(t_{k-1})) = \begin{cases} \boldsymbol{\sigma}^{tr} & \text{if } q_{tr}(0) \leq 0, \\ p\mathbf{I} + \varrho\mathbf{n}^{tr} & \text{if } q_{tr}(0) > 0, \quad q_{tr}(\sqrt{6}\bar{f}_c\varrho^{tr}/2Gm_0) < 0, \\ \frac{\bar{f}_c}{m_0}\mathbf{I} & \text{if } q_{tr}(\sqrt{6}\bar{f}_c\varrho^{tr}/2Gm_0) \geq 0, \end{cases} \quad (4.13)$$

where the function  $q_{tr}$  is defined by (4.8) and  $p$ ,  $\varrho$  are components of the solution to (4.10).

**Theorem 4.3.** *The function  $\mathbf{T}$  is strongly semismooth in  $\mathbb{R}_{sym}^{3 \times 3}$  with respect to  $\boldsymbol{\varepsilon}$ .*

*Proof.* Consider the function  $\Delta\lambda = \Delta\lambda(\boldsymbol{\sigma}^{tr})$  satisfying  $\Delta\lambda = 0$  if  $q_{tr}(0) \leq 0$ , otherwise  $q_{tr}(\Delta\lambda) = 0$ . To apply Theorem 2.1 on the implicit function  $q_{tr}(\gamma) := q(\gamma; p^{tr}, \varrho^{tr})$ , it is necessary to show that  $q$  is strongly semismooth w.r.t. the variables  $\gamma, p^{tr}, \varrho^{tr}$ . This follows from (4.7) and Proposition 2.1. The rest of the proof coincides with the proof of Theorem 3.3.  $\square$

If  $q_{tr}(0) = 0$  or  $q_{tr}(\sqrt{6}\bar{f}_c\varrho^{tr}/2Gm_0) = 0$  then  $\mathbf{T}$  is not smooth. We derive the derivative  $\partial\boldsymbol{\sigma}/\partial\boldsymbol{\varepsilon}$  under the assumption that any of these conditions does not hold. If  $q_{tr}(0) < 0$  (elastic response) then  $\partial\boldsymbol{\sigma}/\partial\boldsymbol{\varepsilon} = \mathbb{D}_e$ . If  $q_{tr}(\sqrt{6}\bar{f}_c\varrho^{tr}/2Gm_0) > 0$  (return to the apex) then  $\partial\boldsymbol{\sigma}/\partial\boldsymbol{\varepsilon} = \mathbb{O}$  (vanishes).

Let  $q_{tr}(0) > 0$  and  $q_{tr}(\sqrt{6}\bar{f}_c\varrho^{tr}/2Gm_0) < 0$ , i.e., return to the smooth portion happens. Then the derivative  $\partial\boldsymbol{\sigma}/\partial\boldsymbol{\varepsilon}$  can be found as follows.

1. Find the solution  $(p, \varrho, \Delta\lambda)$  to (4.10).

2. Use (2.4), (2.5), (3.2) and the chain rule and compute:

$$\begin{aligned} \frac{\partial p^{tr}}{\partial \boldsymbol{\varepsilon}} &= K \mathbf{I}, & \frac{\mathbf{s}^{tr}}{\partial \boldsymbol{\varepsilon}} &= 2G \mathbb{I}_{dev}, & \frac{\partial \varrho^{tr}}{\partial \boldsymbol{\varepsilon}} &= 2G \mathbf{n}^{tr}, & \frac{\partial \mathbf{n}^{tr}}{\partial \boldsymbol{\varepsilon}} &= \frac{2G}{\varrho^{tr}} (\mathbb{I}_{dev} - \mathbf{n}^{tr} \otimes \mathbf{n}^{tr}), \\ \frac{\partial \theta^{tr}}{\partial \boldsymbol{\varepsilon}} &= \frac{2G\sqrt{6}}{\varrho^{tr} \sin(3\theta^{tr})} [(\mathbf{n}^{tr} \otimes (\mathbf{n}^{tr})^3) \mathbf{I} - \mathbb{I}_{dev}(\mathbf{n}^{tr})^2], & \frac{\partial r_e^{tr}}{\partial \boldsymbol{\varepsilon}} &= -r_e'(\cos \theta^{tr}) \sin \theta^{tr} \frac{\partial \theta^{tr}}{\partial \boldsymbol{\varepsilon}}. \end{aligned}$$

3. Compute:

$$\begin{pmatrix} \frac{\partial p}{\partial \boldsymbol{\varepsilon}} \\ \frac{\partial \varrho}{\partial \boldsymbol{\varepsilon}} \\ \frac{\partial \Delta \lambda}{\partial \boldsymbol{\varepsilon}} \end{pmatrix} = \begin{pmatrix} 1 + \Delta \lambda K \frac{m_g''(p)}{f_c} & 0 & K \frac{m_g'(p)}{f_c} \\ 0 & 1 + \Delta \lambda \frac{6G}{f_c^2} & 2G \left( \frac{3\varrho}{f_c^2} + \frac{m_0}{\sqrt{6}f_c} \right) \\ \frac{m_0}{f_c} & \frac{3\varrho}{f_c^2} + \frac{m_0 r_e^{tr}}{\sqrt{6}f_c} & 0 \end{pmatrix}^{-1} \begin{pmatrix} \frac{\partial p^{tr}}{\partial \boldsymbol{\varepsilon}} \\ \frac{\partial \varrho^{tr}}{\partial \boldsymbol{\varepsilon}} \\ -\frac{m_0 \varrho}{\sqrt{6}f_c} \frac{\partial r_e^{tr}}{\partial \boldsymbol{\varepsilon}} \end{pmatrix}. \quad (4.14)$$

Notice that the matrix in (4.14) arises from linearization of (4.10) around the solution  $(p, \varrho, \Delta \lambda)$ . The matrix is invertible since its determinant is negative.

4. Compute

$$\frac{\partial \boldsymbol{\sigma}}{\partial \boldsymbol{\varepsilon}} = \mathbf{I} \otimes \frac{\partial p}{\partial \boldsymbol{\varepsilon}} + \mathbf{n}^{tr} \otimes \frac{\partial \varrho}{\partial \boldsymbol{\varepsilon}} + \varrho \frac{\partial \mathbf{n}^{tr}}{\partial \boldsymbol{\varepsilon}}. \quad (4.15)$$

For numerical purposes, we use the following generalized consistent tangent operator:

$$\mathbb{T}^o(\boldsymbol{\varepsilon}; \boldsymbol{\varepsilon}^p(t_{k-1})) = \begin{cases} \mathbb{D}_e & \text{if } q_{tr}(0) \leq 0, \\ (4.15) & \text{if } q_{tr}(0) > 0, \quad q_{tr}(\sqrt{6}f_c \varrho^{tr}/2Gm_0) < 0, \\ \mathbb{O} & \text{if } q_{tr}(\sqrt{6}f_c \varrho^{tr}/2Gm_0) \geq 0. \end{cases} \quad (4.16)$$

## 5 An abstract model

The aim of this section is an extension of Theorem 3.1 and 4.1 on a specific class of elastoplastic models that are usually formulated in the Haigh-Westergaard coordinates. We consider an abstract model containing the isotropic hardening and the plastic flow pseudo-potential. *Given the history of the strain tensor  $\boldsymbol{\varepsilon} = \boldsymbol{\varepsilon}(t)$ ,  $t \in [t_0, t_{\max}]$ , and the initial values*

$$\boldsymbol{\varepsilon}^p(t_0) = \boldsymbol{\varepsilon}^p, \quad \bar{\boldsymbol{\varepsilon}}^p(t_0) = \bar{\boldsymbol{\varepsilon}}_0^p.$$

*Find the generalized stress  $(\boldsymbol{\sigma}(t), \kappa(t))$  and the generalized strain  $(\boldsymbol{\varepsilon}^p(t), \bar{\boldsymbol{\varepsilon}}^p(t))$  such that*

$$\left. \begin{aligned} \boldsymbol{\varepsilon} &= \boldsymbol{\varepsilon}^e + \boldsymbol{\varepsilon}^p, \\ \boldsymbol{\sigma} &= \mathbb{D}_e : \boldsymbol{\varepsilon}^e, \quad \kappa = H(\bar{\boldsymbol{\varepsilon}}^p), \\ \dot{\boldsymbol{\varepsilon}}^p &\in \dot{\lambda} \partial_{\boldsymbol{\sigma}} g(\boldsymbol{\sigma}, \kappa), \\ \dot{\bar{\boldsymbol{\varepsilon}}}^p &= \dot{\lambda} \ell(\boldsymbol{\sigma}, \kappa), \\ \dot{\lambda} &\geq 0, \quad f(\boldsymbol{\sigma}, \kappa) \leq 0, \quad \dot{\lambda} f(\boldsymbol{\sigma}, \kappa) = 0. \end{aligned} \right\}$$

*hold for each instant  $t \in [t_0, t_{\max}]$ .*

Further, we have the following assumptions on ingredients of the model:

1.  $f(\boldsymbol{\sigma}, \kappa) = \hat{f}(p(\boldsymbol{\sigma}), \varrho(\boldsymbol{\sigma}), \varrho_e(\boldsymbol{\sigma}), \kappa)$ , where  $\hat{f}$  is increasing with respect to  $\varrho$  and  $\tilde{\varrho}$ , convex and continuously differentiable at least in vicinity of the yield surface.
2.  $g(\boldsymbol{\sigma}, \kappa) = \hat{g}(p(\boldsymbol{\sigma}), \varrho(\boldsymbol{\sigma}), \kappa)$ , where  $\hat{g}$  is an increasing function with respect to  $\varrho$ , convex and twice continuously differentiable at least in vicinity of the yield surface.



3.  $H$  is a nondecreasing, continuous and strongly semismooth function satisfying  $H(0) = 0$ .
4.  $\ell(\boldsymbol{\sigma}, \kappa) = \hat{\ell}(p(\boldsymbol{\sigma}), \varrho(\boldsymbol{\sigma}), \tilde{\varrho}(\boldsymbol{\sigma}), \kappa)$  is a positive function.
5. Invariants  $p, \varrho, \varrho_e$  and  $\tilde{\varrho}$  are the same as in Section 2.

Notice that the assumptions on  $\hat{f}$  and  $\hat{g}$  guarantee convexity of  $f$  and  $g$  using properties of  $r_e$  introduced in [39]. Let  $\hat{g}_V(p, \varrho) := \frac{\partial \hat{g}}{\partial p}$ ,  $\hat{g}_\varrho(p, \varrho) := \frac{\partial \hat{g}}{\partial \varrho}$ . Then one can write the plastic flow rule as follows:

$$\dot{\boldsymbol{\varepsilon}}^p = \dot{\lambda} [\hat{g}_V(p, \varrho) \mathbf{I} / 3 + \hat{g}_\varrho(p, \varrho) \hat{\mathbf{n}}], \quad \hat{\mathbf{n}} \in \partial \varrho(\boldsymbol{\sigma}).$$

The  $k$ -th step of the incremental constitutive problem received by the implicit Euler method reads as follows. *Given  $\boldsymbol{\varepsilon} := \boldsymbol{\varepsilon}(t_k)$ ,  $\boldsymbol{\sigma}^{tr} := \mathbb{D}_e : (\boldsymbol{\varepsilon}(t_k) - \boldsymbol{\varepsilon}^p(t_{k-1}))$  and  $\bar{\boldsymbol{\varepsilon}}^{p,tr} := \bar{\boldsymbol{\varepsilon}}^p(t_{k-1})$ . Find  $\boldsymbol{\sigma} = \boldsymbol{\sigma}(t_k)$ ,  $\bar{\boldsymbol{\varepsilon}}^p = \bar{\boldsymbol{\varepsilon}}^p(t_k)$  and  $\Delta\lambda$  satisfying:*

$$\left. \begin{aligned} \boldsymbol{\sigma} &= \boldsymbol{\sigma}^{tr} - \Delta\lambda [K \hat{g}_V(p(\boldsymbol{\sigma}), \varrho(\boldsymbol{\sigma})) \mathbf{I} + 2G \hat{g}_\varrho(p(\boldsymbol{\sigma}), \varrho(\boldsymbol{\sigma})) \hat{\mathbf{n}}], \quad \hat{\mathbf{n}} \in \partial \varrho(\boldsymbol{\sigma}), \\ \bar{\boldsymbol{\varepsilon}}^p &= \bar{\boldsymbol{\varepsilon}}^{p,tr} + \Delta\lambda \ell(\boldsymbol{\sigma}, \kappa), \\ \Delta\lambda &\geq 0, \quad f(\boldsymbol{\sigma}, H(\bar{\boldsymbol{\varepsilon}}^p)) \leq 0, \quad \Delta\lambda f(\boldsymbol{\sigma}, H(\bar{\boldsymbol{\varepsilon}}^p)) = 0. \end{aligned} \right\} \quad (5.1)$$

If we use the elastic predictor/plastic corrector method then we derive the following straightforward extension of Theorem 3.1 and Theorem 4.1 within the plastic correction.

**Theorem 5.1.** *Let  $f(\boldsymbol{\sigma}^{tr}, H(\bar{\boldsymbol{\varepsilon}}^{p,tr})) > 0$ . If  $(\boldsymbol{\sigma}, \bar{\boldsymbol{\varepsilon}}^p, \Delta\lambda)$  is a solution to problem (5.1) then  $(p, \varrho, \bar{\boldsymbol{\varepsilon}}^p, \Delta\lambda)$ ,  $\Delta\lambda > 0$ , is a solution to the following system:*

$$\left. \begin{aligned} p &= p^{tr} - \Delta\lambda K \hat{g}_V(p, \varrho), \\ \varrho &= [\varrho^{tr} - \Delta\lambda 2G \hat{g}_\varrho(p, \varrho)]^+, \\ \bar{\boldsymbol{\varepsilon}}^p &= \bar{\boldsymbol{\varepsilon}}^{p,tr} + \Delta\lambda \hat{\ell}(p, \varrho, \varrho \tilde{r}(\cos \theta^{tr})), \\ \hat{f}(p, \varrho, \varrho r_e(\cos \theta^{tr}), H(\bar{\boldsymbol{\varepsilon}}^p)) &= 0. \end{aligned} \right\} \quad (5.2)$$

Conversely, if  $(p, \varrho, \kappa, \Delta\lambda)$  is a solution to (5.2) then  $(\boldsymbol{\sigma}, \kappa, \Delta\lambda)$  solves (5.1), where

$$\boldsymbol{\sigma} = \begin{cases} p \mathbf{I} + \varrho \mathbf{n}^{tr} & \text{if } \varrho > 0, \\ p \mathbf{I} & \text{if } \varrho = 0. \end{cases} \quad (5.3)$$

Notice that it is generally impossible to a priori decide about the type of the return as in the models introduced above. To be in accordance with the current approach introduced e.g. in [15] one can split (5.2) into the following two systems:

$$\left. \begin{aligned} p + \Delta\lambda K \hat{g}_V(p, 0) &= p^{tr} \\ \bar{\boldsymbol{\varepsilon}}^p - \Delta\lambda \hat{\ell}(p, 0, 0) &= \bar{\boldsymbol{\varepsilon}}^{p,tr} \\ \hat{f}(p, 0, 0, H(\bar{\boldsymbol{\varepsilon}}^p)) &= 0 \end{aligned} \right\} \quad \text{for } \varrho = 0 \text{ (return to the apex (apices)),} \quad (5.4)$$

$$\left. \begin{aligned} p + \Delta\lambda K \hat{g}_V(p, \varrho) &= p^{tr} \\ \varrho + \Delta\lambda 2G \hat{g}_\varrho(p, \varrho) &= \varrho^{tr} \\ \bar{\boldsymbol{\varepsilon}}^p - \Delta\lambda \hat{\ell}(p, \varrho, \varrho \tilde{r}(\cos \theta^{tr})) &= \bar{\boldsymbol{\varepsilon}}^{p,tr} \\ \hat{f}(p, \varrho, \varrho r_e(\cos \theta^{tr}), H(\bar{\boldsymbol{\varepsilon}}^p)) &= 0 \end{aligned} \right\} \quad \text{for } \varrho > 0 \text{ (return to the smooth portion),} \quad (5.5)$$

and guess which of these systems provides an admissible solution. Beside the blind guessing, the current approach has another drawback: it can happen that (5.2) has a unique solution and mutually one of the systems (5.4), (5.5) does not have any solution or have more than one solution. Therefore, we recommend to solve (5.2) directly by a nonsmooth version of the Newton method with the standard initial choice  $p^0 = p^{tr}$ ,  $\varrho^0 = \varrho^{tr}$ ,  $\kappa^0 = \kappa^{tr}$  and  $\Delta\lambda^0 = 0$ .

## 6 Numerical realization of the incremental boundary value elastoplastic problem

Consider an elasto-plastic body occupying a bounded domain  $\Omega \subseteq \mathbb{R}^3$  with the Lipschitz continuous boundary  $\Gamma$ . It is assumed that  $\Gamma = \bar{\Gamma}_D \cup \bar{\Gamma}_N$ , where  $\Gamma_D$  and  $\Gamma_N$  are open and disjoint sets. On  $\Gamma_D$ , the homogeneous Dirichlet boundary condition is prescribed. Surface tractions of density  $\mathbf{f}_t$  are applied on  $\Gamma_N$  and the body is subject to a volume force  $\mathbf{f}_V$ .

Notice that the above defined stress, strain and hardening variables depend on the spatial variable  $\mathbf{x} \in \Omega$ , i.e.  $\boldsymbol{\sigma}_k = \boldsymbol{\sigma}_k(\mathbf{x})$ , etc. Let  $\mathcal{V} := \{\mathbf{v} \in [H^1(\Omega)]^3 \mid \mathbf{v} = \mathbf{0} \text{ on } \Gamma_D\}$  denote the space of kinematically admissible displacements. Under the infinitesimal small strain assumption, we have  $\boldsymbol{\varepsilon}(\mathbf{v}) = \frac{1}{2}(\nabla \mathbf{v} + (\nabla \mathbf{v})^T)$ ,  $\mathbf{v} \in \mathcal{V}$ .

Substitution of the stress-strain operator  $\mathbf{T}$  into the principle of the virtual work leads to the following problem at the  $k$ -th step:

$$(P_k) \quad \text{find } \mathbf{u}_k \in \mathcal{V} : \quad \int_{\Omega} \mathbf{T}(\boldsymbol{\varepsilon}(\mathbf{u}_k); \boldsymbol{\varepsilon}_{k-1}^p, \bar{\boldsymbol{\varepsilon}}_{k-1}^p) : \boldsymbol{\varepsilon}(\mathbf{v}) \, d\Omega = \int_{\Omega} \mathbf{f}_{V,k} \cdot \mathbf{v} \, d\Omega + \int_{\Gamma_N} \mathbf{f}_{t,k} \cdot \mathbf{v} \, d\Gamma \quad \forall \mathbf{v} \in \mathcal{V},$$

where  $\mathbf{f}_{V,k}$  and  $\mathbf{f}_{t,k}$  are the prescribed volume, and surface forces at  $t_k$ , respectively. After finding a solution  $\mathbf{u}_k$ , the remaining unknown fields  $\boldsymbol{\varepsilon}_k^p, \bar{\boldsymbol{\varepsilon}}_k^p$  important for the next step can be computed at the level of integration points. Problem  $(P_k)$  can be standardly written as the operator equation in the dual space  $\mathcal{V}'$  to  $\mathcal{V}$ :  $\mathcal{F}_k(\mathbf{u}_k) = \ell_k$ , where

$$\begin{aligned} \langle \mathcal{F}_k(\mathbf{u}), \mathbf{v} \rangle &= \int_{\Omega} \mathbf{T}(\boldsymbol{\varepsilon}(\mathbf{u}); \boldsymbol{\varepsilon}_{k-1}^p, \bar{\boldsymbol{\varepsilon}}_{k-1}^p) : \boldsymbol{\varepsilon}(\mathbf{v}) \, d\Omega \quad \forall \mathbf{u}, \mathbf{v} \in \mathcal{V}, \\ \langle \ell_k, \mathbf{v} \rangle &= \int_{\Omega} \mathbf{f}_{V,k} \cdot \mathbf{v} \, d\Omega + \int_{\Gamma_N} \mathbf{f}_{t,k} \cdot \mathbf{v} \, d\Gamma \quad \forall \mathbf{v} \in \mathcal{V}. \end{aligned}$$

Since we plan to use the semismooth Newton method, we also introduce the operator  $\mathcal{K}_k : \mathcal{V} \rightarrow \mathcal{L}(\mathcal{V}, \mathcal{V}')$  as follows:

$$\langle \mathcal{K}_k(\mathbf{u})\mathbf{v}, \mathbf{w} \rangle = \int_{\Omega} \mathbb{T}^o(\boldsymbol{\varepsilon}(\mathbf{u}); \boldsymbol{\varepsilon}_{k-1}^p, \bar{\boldsymbol{\varepsilon}}_{k-1}^p) \boldsymbol{\varepsilon}(\mathbf{v}) : \boldsymbol{\varepsilon}(\mathbf{w}) \, d\Omega \quad \forall \mathbf{u}, \mathbf{v}, \mathbf{w} \in \mathcal{V}.$$

To discretize the problem in space we use the finite element method. Then the space  $\mathcal{V}$  is approximated by a finite dimensional one,  $\mathcal{V}_h$ . If linear simplicial elements are not used then it is also necessary to consider a suitable numerical quadrature on each element. Let  $\mathcal{F}_{k,h}, \mathcal{K}_{k,h}, \ell_{k,h}$  denote the approximation of operators  $\mathcal{F}_k, \mathcal{K}_k, \ell_k$ , respectively, and  $\mathbf{F}_k : \mathbb{R}^n \rightarrow \mathbb{R}^n$ ,  $\mathbf{K}_k : \mathbb{R}^n \rightarrow \mathbb{R}^{n \times n}$ ,  $\mathbf{l}_k \in \mathbb{R}^n$  be their algebraic counterparts. Then the discretization of problem  $(P_k)$  leads to the system of nonlinear equations,  $\mathbf{F}_k(\mathbf{u}_k) = \mathbf{l}_k$ , and the semismooth Newton method reads as follows:

*Algorithm 1* (Semismooth Newton method).

- 1: initialization:  $\mathbf{u}_k^0 = \mathbf{u}_{k-1}$
- 2: **for**  $i = 0, 1, 2, \dots$  **do**
- 3:   find  $\delta \mathbf{u}^i \in \mathcal{V}$ :  $\mathbf{K}_k(\mathbf{u}_k^i) \delta \mathbf{u}^i = \mathbf{l}_k - \mathbf{F}_k(\mathbf{u}_k^i)$
- 4:   compute  $\mathbf{u}_k^{i+1} = \mathbf{u}_k^i + \delta \mathbf{u}^i$
- 5:   **if**  $\|\delta \mathbf{u}^i\| / (\|\mathbf{u}_k^{i+1}\| + \|\mathbf{u}_k^i\|) \leq \epsilon_{Newton}$  **then stop**
- 6: **end for**
- 7: set  $\mathbf{u}_k = \mathbf{u}_k^{i+1}$ .

If  $\mathbf{T}$  is strongly semismooth in  $\mathbb{R}^{3 \times 3}_{sym}$  then  $\mathbf{F}_k$  is strongly semismooth in  $\mathbb{R}^n$ . Notice that the strong semismoothness is an essential assumption for local quadratic convergence of this algorithm. In numerical examples introduced below, we observe local quadratic convergence when the tolerance is sufficiently small. In particular, we set  $\epsilon_{Newton} = 10^{-12}$ .

## 7 Numerical example - slope stability

The improved return-mapping schemes in combination with the semismooth Newton method have been partially implemented in codes SIFEL [1] and MatSol [21]. Here, for the sake of simplicity, we consider the slope stability benchmark [11, Page 351] for the presented models, the Drucker-Prager (DP) and the Jirasek-Grassl (JG) ones. The benchmark is formulated as a plane strain problem. We focus on: a) incremental limit analysis and b) dependence of loading paths on element types and mesh density. For purposes of such an experiment, special MatLab codes have been prepared to be transparent. These experimental codes are available in [2] together with selected graphical outputs.

The geometry of the body is depicted in Figure 2 or 3. The slope height is 10 m and its inclination is  $45^\circ$ . On the bottom, we assume that the body is fixed and, on the left and right sides, zero normal displacements are prescribed. The body is subjected to self-weight. We set the specific weight  $\rho g = 20 \text{ kN/m}^3$  with  $\rho$  being the mass density and  $g$  the gravitational acceleration. Such a volume force is multiplied by a scalar factor,  $\zeta$ . The loading process starts from  $\zeta = 0$ . The gravity load factor,  $\zeta$ , is then increased gradually until collapse occurs. The initial increment of the factor is set to 0.1. To illustrate loading responses we compute settlement at the corner point  $A$  on the top of the slope depending on  $\zeta$ .

As in [11, Page 351], we set  $E = 20\,000 \text{ kPa}$ ,  $\nu = 0.49$ ,  $\phi = 20^\circ$  and  $c = 50 \text{ kPa}$ , where  $c$  denotes the cohesion for the perfect plastic model. Hence,  $G = 67\,114 \text{ kPa}$  and  $K = 3\,333\,333 \text{ kPa}$ . In comparison to [11], we use the presented models instead of the Mohr-Coulomb one. The remaining parameters for these models will be introduced below.

We analyze the problem for linear triangular ( $P1$ ) elements and eight-pointed quadrilateral ( $Q2$ ) elements. In the latter case,  $(3 \times 3)$ -point Gauss quadrature is used. For each element type, a hierarchy of four meshes with different densities is considered. The  $P1$ -meshes contain 3210, 12298, 48126, and 190121 nodal points, respectively. The  $Q2$ -meshes consist of 627, 2405, 9417, and 37265 nodal points, respectively. The coarsest meshes for  $P1$  and  $Q2$  elements are depicted in Figure 2 and 3. Let us complete that the mesh in Figure 2 is uniform in vicinity of the slope and consists of right isosceles triangles with the same diagonal orientation. Further, it is worth mentioning that the  $P1$ -meshes are chosen much more finer in vicinity of the slope than their  $Q2$ -counterparts within the same level.

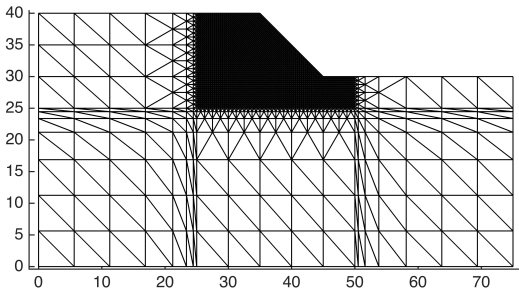


Figure 2: The coarsest mesh for  $P1$  elements.

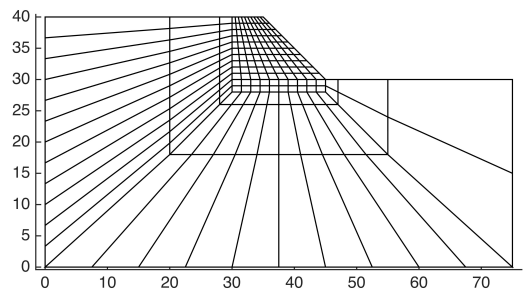


Figure 3: The coarsest mesh for  $Q2$  elements.

### 7.1 The Drucker-Prager model

The Drucker-Prager parameters  $\eta$ ,  $\bar{\eta}$  and  $\xi$  are computed from the friction angle,  $\phi$ , and the dilatancy angle,  $\psi$ , as follows [11]:

$$\eta = \frac{3 \tan \phi}{\sqrt{9 + 12(\tan \phi)^2}}, \quad \bar{\eta} = \frac{3 \tan \psi}{\sqrt{9 + 12(\tan \psi)^2}}, \quad \xi = \frac{3}{\sqrt{9 + 12(\tan \phi)^2}}.$$

At first, we introduce results obtained for the model with associative perfect plasticity. In such a case,  $\psi = \phi$ ,  $c_0 = c$  and  $H = 0$  kPa. The received loading curves for the investigated meshes and elements are depicted in Figure 4 and 5. Although  $P1$ -meshes are much finer, we observe more significant dependence of the curves on the mesh density for  $P1$ -elements than for  $Q2$ -elements. Also computed limit load factors are greater and tend more slowly to a certain value as  $h \rightarrow 0_+$  for  $P1$ -meshes than for  $Q2$ -meshes. The expected limit value is 4.045 as follows from considerations introduced in [7]. Using the finest  $P1$  and  $Q2$  meshes, we receive the values 4.230, and 4.056, respectively.

In general, higher order elements are recommended when a locking effect is expected. In this example, it can be caused due to the presence of the limit load and/or  $\nu \approx 1/2$ . On the other hand, the strong dependence on mesh density is influenced by other factors like mesh structure or choice of a model. For example, this dependence is not so significant for the Jirasek-Grassl model (see the next subsection). Further, in [19], there is theoretically justified and illustrated that the dependence of the limit load on the mesh density is minimal for bounded yield surfaces and that an approximation of unbounded yield surfaces by bounded ones (the truncation) leads to a lower bound of the limit load.

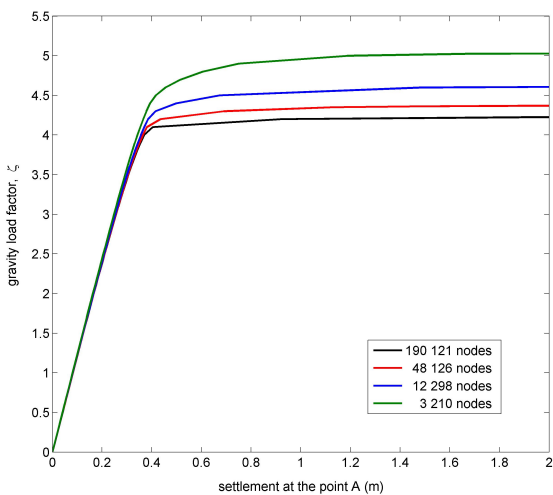


Figure 4: Loading paths for the associative perfect plastic model and  $P1$  elements.

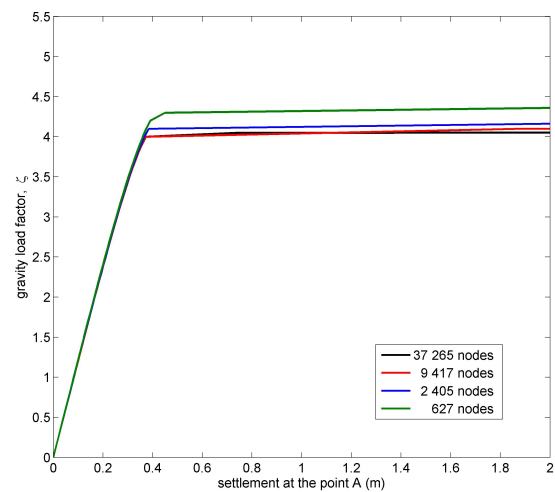


Figure 5: Loading paths for the associative perfect plastic model and  $Q2$  elements.

For illustration, we add Figure 6 and 7 with plastic multipliers and total displacements at collapse, respectively. The figures are in accordance with literature.

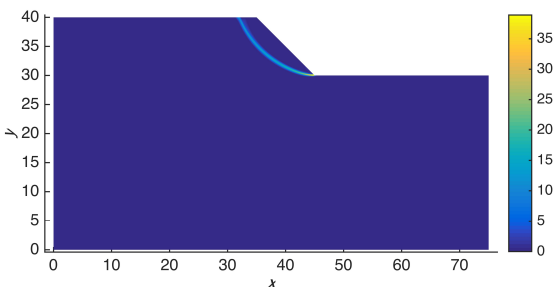


Figure 6: Plastic multipliers at collapse for the finest  $Q2$ -mesh.

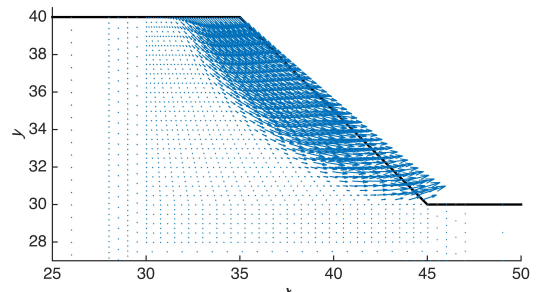


Figure 7: Displacements at collapse (detail) for the  $Q2$ -mesh with 2405 nodes.

To compare the current return-mapping scheme with improved one, we have also considered the

nonassociative model with nonlinear hardening where

$$\psi = 10^\circ, c_0 = 40 \text{ kPa}, \tilde{H} = 10000 \text{ kPa}, H(\bar{\varepsilon}^p) = \min \left\{ c - c_0, \tilde{H}\bar{\varepsilon}^p - \frac{\tilde{H}^2}{4(c - c_0)}(\bar{\varepsilon}^p)^2 \right\}.$$

Here,  $\tilde{H}$  represents the initial slope of the hardening function and the material response is perfect plastic for sufficiently large values of the hardening variable. This nonassociative model yields a slightly lower values of the limit load factors and also the other results are very similar to the associative model. The related graphical outputs are available in [2, SS-DP-NH]. Further, in vicinity of the limit load, we have observed lower rounding errors for the improved return-mapping scheme and thus lower number of Newton steps is necessary to receive the prescribe tolerance than for the current scheme. However, the computational time for both schemes are practically the same since return to the apex happens only on a few elements lying in vicinity of the yield surface.

## 7.2 The simplified Jirasek-Grassl model

To be the simplified Jirasek-Grassl (JG) model applicable for the investigated soil material we fit its parameters using the associative perfect plastic Drucker-Prager (DP) model as follows:  $e = 1$ ,  $\bar{f}_c = 3c\xi/(\sqrt{3} - \eta)$ ,  $\bar{f}_t = 0$ ,  $B_g = 1000$ ,  $s = 5$ ,  $A_g = s\eta$  and  $m_0 = \sqrt{3}s - 6$ . Recall that  $e = 1$  implies  $\varrho_e = \varrho$ . Further the value of  $\bar{f}_c$  corresponds to the uniaxial compressive strength computed from the Drucker-Prager model. To eliminate the influence of the exponential term in the function  $m_g$ , the value of  $B_g$  is chosen sufficiently large. Then the model is insensitive on  $\bar{f}_t$  and one can vanish it. Finally, we require the same flow direction for both the models under the uniaxial compressive strength. Since the yield function in the JG model is normalized in comparison to the DP model it is convenient to introduce the following relation between the plastic multipliers:  $\Delta\lambda_{DP} = \frac{s}{\bar{f}_c}\Delta\lambda_{JG}$ , where  $s$  is a scale factor. Then the values of  $m_0$  and  $A_g$  are determined from the following equations:

$$s\eta = m'_g(\bar{f}_c/3) \approx A_g, \quad \frac{s}{\sqrt{2}} = \sqrt{6} + \frac{m_0}{\sqrt{6}}.$$

To be  $m_0$  positive,  $s$  must be greater than  $2\sqrt{3}$ . To be in accordance with results of the DP model, we set  $s = 4.9$ .<sup>1</sup> Comparison of yield surfaces (in the meridian plane) and flow directions for the DP and JG models is illustrated in Figure 8. Here, the fixed value  $\Delta\lambda_{DP} = 0.001$  is used for vectors representing the flow directions.

Loading curves for the investigated  $P1$ ,  $Q2$  meshes and the JG model are depicted in Figure 9 and 10. We observe much faster convergence of the  $P1$ -loading curves than for the DP model. Moreover, the results for  $P1$  and  $Q2$  elements are comparable. The computed values of the limit load factor on the finest  $P1$  and  $Q2$  meshes are 4.124, and 4.107, respectively.

## 8 Conclusion

The main idea of this paper is that the subdifferential formulation of the plastic flow rule is also useful for computational purposes and numerical analysis. Namely, it has been shown that such an approach improves the implicit return-mapping scheme for non-smooth plastic pseudo-potentials as follows.

- The unique system of nonlinear equations is solved regardless on a type of the return.

<sup>1</sup>For smaller values of  $s$ , the limit load factor is underestimated and for greater values of  $s$  the limit load factor is overestimated.

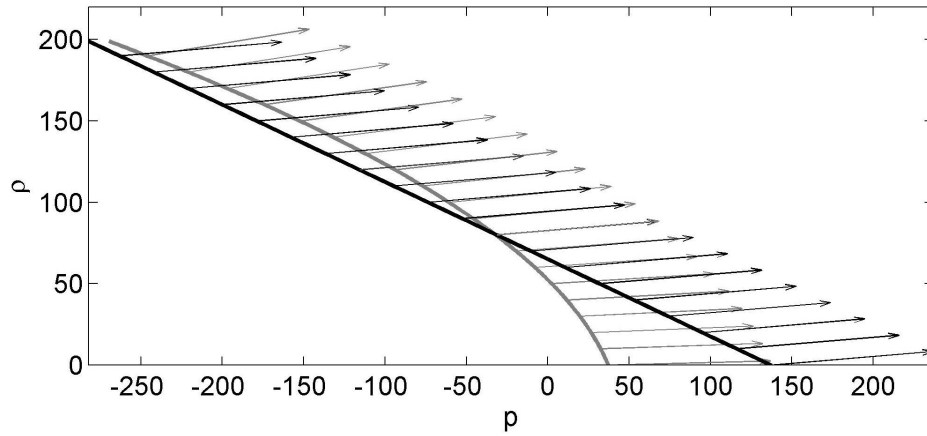


Figure 8: Comparison of the yield surfaces (in the meridian plane) and the flow directions for the DP model (black) and the JG model (grey).

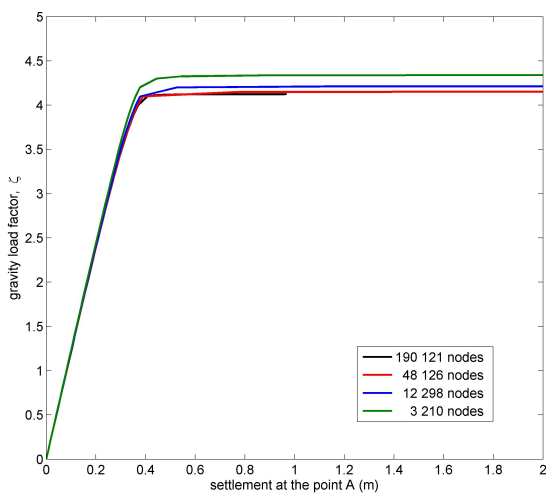


Figure 9:  $P1$  - loading paths for the simplified Jirasek-Grassl model.

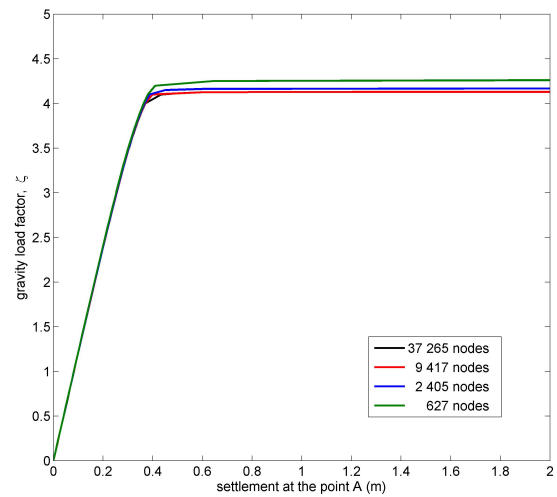


Figure 10:  $Q2$  - loading paths for the simplified Jirasek-Grassl model.

- It can be a priori determined the type of the return from a given trial state for some models (without knowledge of the solution).
- The scheme can be more correct than the current one, and its form enables to study properties of constitutive operators like existence, uniqueness and semismoothness.

In this paper (PART I), the new technique has been systematically built on a specific class of models containing singularities only along the hydrostatic axis. Beside an abstract model, two particular models have been studied: The Drucker-Prager and the simplified Jirasek-Grassl model. However, the presented idea seems to be more universal. For example, it has been successfully used for the Mohr-Coulomb model in "PART II" [37].

## Acknowledgements

The authors would like to thank to Pavel Maršálek for generating the quadrilateral meshes with mid-points. This work has been supported by the project 13-18652S (GA CR) and the European Regional Development Fund in the IT4Innovations Centre of Excellence project (CZ.1.05/1.1.00/02.0070).

## References

- [1] SIFEL home page. <http://mech.fsv.cvut.cz/~sifel>, 2001-2015.
- [2] Experimental Matlab code for the slope stability benchmark. [www.ugm.cas.cz/?p=publish/output.php](http://www.ugm.cas.cz/?p=publish/output.php) (or [www.ugm.cas.cz](http://www.ugm.cas.cz) - Publications - Other outputs - SS-DP-AP, SS-DP-NH, SS-JG-P), 2015.
- [3] Armero F, Pérez-Foguet A. On the Formulation of Closest-Point Projection Algorithms in Elastoplasticity - Part I: The Variational Structure. *International Journal for Numerical Methods in Engineering* 2002; **53**: 297-329.
- [4] Blaheta R. Convergence of Newton-type methods in incremental return mapping analysis of elastoplastic problems. *Comput. Methods Appl. Mech. Engrg.* 1997 **147**:167-185.
- [5] Caddemi S, Martin JB. Convergence of the Newton-Raphson Algorithm in Elastic-plastic Incremental Analysis. *International Journal for Numerical Methods in Engineering* 1991; **31**: 177-191.
- [6] Cermak M, Kozubek T, Sysala S, Valdman J. A TFETI Domain Decomposition Solver for Elastoplastic Problems. *Applied Mathematics and Computation* 2014; **231**: 634-653.
- [7] Chen W, Liu XL. *Limit Analysis in Soil Mechanics*. Elsevier, 1990.
- [8] Clarke HF. *Optimization and Nonsmooth Analysis*. Wiley, New York, 1983.
- [9] De Angelis F, Taylor RL. An efficient return mapping algorithm for elastoplasticity with exact closed form solution of the local constitutive problem, *Engineering Computations* 2015; **32**: 2259 - 2291.
- [10] de Saxcé G. The bipotential method, a new variational and numerical treatment of the dissipative laws of materials. In: *10th. Int. Conf. on Mathematical and Computer Modelling and Scientific Computing*, pp. 1-6, 1995.
- [11] de Souza Neto EA, Perić D, Owen DRJ. *Computational methods for plasticity: theory and application*. Wiley, 2008.
- [12] Facchinei F, Pang JS. Finite-Dimensional Variational Inequalities and Complementarity Problems, vol. II, in: *Springer Series in Operations Research*, Springer, New York, 2003.
- [13] Feijóo RA, Zouain N. Formulations in Rates and Increments for Elastic-plastic Analysis. *International Journal for Numerical Methods in Engineering* 1988; **26**: 2031-2048.

- [14] Gowda MS. Inverse and implicit function theorem for H-differentiable and semismooth functions. *Optim. Methods Softw.* 2004; **19**: 443–461.
- [15] Grassl P, Jirásek M. Damage-plastic model for concrete failure. *International Journal of Solids and Structure* 2006; **43**: 7166-7196.
- [16] Gruber PG, Valdman J. Solution of One-Time Step Problems in Elastoplasticity by a Slant Newton Method. *SIAM J. Sci. Comput.* 2009; **31**: 1558–1580.
- [17] Gurtin ME. *An Introduction to Continuum Mechanics*. Academic Press: Orlando, 1981.
- [18] Han W, Reddy BD. *Plasticity: mathematical theory and numerical analysis*. Springer, 1999.
- [19] Haslinger J, Repin S, Sysala S. Guaranteed and computable bounds of the limit load for variational problems with linear growth energy functionals. Submitted, 2015.
- [20] Hjaaj M, Fortin J, de Saxcé G. A complete stress update algorithm for the non-associated Drucker-Prager model including treatment of the apex. *International Journal of Engineering Science* 2003 **41**: 1109-1143.
- [21] Kozubek T, Markopoulos A, Brzobohatý T, Kučera R, Vondrák V, Dostál Z. *MatSol - MATLAB efficient solvers for problems in engineering*, <http://matsol.vsb.cz/>.
- [22] Menétrey P, Willam KJ. A triaxial failure criterion for concrete and its generalization. *ACI Structural Journal* 1995; **92**, 311-318.
- [23] Meng F, Sun D, Zhao G. Semismoothness of solutions to generalized equations and Moreau-Yosida regularization. *Math. Program., Ser. B* 2005; **104**: 561–581.
- [24] Mielke A, Roubíček T. *Rate-Independent Systems: Theory and Application*. (Appl. Math. Sci. Series 193) Springer: New York, 2015, ISBN 978-1-4939-2705-0.
- [25] Mifflin R. Semismoothness and semiconvex function in constraint optimization. *SIAM J. Control Optim.* 1977; **15**: 957–972.
- [26] Pang JS, Sun D, Sun J. Semismoothness Homeomorphisms and Strong Stability of Semidefinite and Lorentz Cone Complementarity Problems. *Math. Oper. Res.* 2003; **28**: 39–63.
- [27] Pérez-Foguet A, Armero F. On the Formulation of Closest-point Projection Algorithms in Elastoplasticity - Part II: Globally Convergent Schemes. *International Journal for Numerical Methods in Engineering* 2002; **53**: 331-374.
- [28] Qi L, Sun J. A nonsmooth version of Newton’s method. *Mathematical Programming* 1993; **58**: 353-367.
- [29] Reddy BD, Martin JB. Algorithms for the Solution of Internal Variable Problems in Plasticity. *Comp. Meth. Appl. Mech. Engng* 1991; **93**: 253-273.
- [30] Rockafellar RT. *Convex analysis*. Princeton University Press: Princeton, New Jersey, 1970.
- [31] Sauter M, Wieners C. On the superlinear convergence in computational elastoplasticity. *Comp. Meth. Eng. Mech.* 2011; **200**: 3646-3658.
- [32] Simo JC, Hughes TJR. *Computational Inelasticity*. Springer-Verlag, New-York, 1998.
- [33] Starman B, Halilović M, Vrh M, Štok B. Consistent tangent operator for cutting-plane algorithm of elasto-plasticity. *Computer Methods in Applied Mechanics and Engineering* 2014; **272**: 214-232.
- [34] Sun D. A further result on an implicit function theorem for locally Lipschitz function. *Oper. Res. Lett.* 2001; **28**: 193–198.



- [35] Sysala S. Application of a modified semismooth Newton method to some elasto-plastic problems. *Math. Comp. Sim.* 2012; **82**: 2004–2021.
- [36] Sysala S. Properties and simplifications of constitutive time-discretized elastoplastic operators. *ZAMM - Z. Angew. Math. Mech.* 2014; **94**: 233-255.
- [37] Sysala S. An improved return-mapping scheme for nonsmooth plastic potentials: PART II - the Mohr-Coulomb yield criterion. Available at <http://arxiv.org/abs/1508.07435>.
- [38] Unteregger D, Hofstetter G. A unified constitutive model for different types of intact rock. *Submitted to International Journal of Rock Mechanics and Mining Science*, 2013.
- [39] Willam KJ, Warnke EP. Constitutive model for the triaxial behavior of concrete. I.: Concrete Structure Subjected to Triaxial Stresses. *Vol. 19 of IABSE Report, International Association of Bridge and Structural Engineers*, Zurich, 1974, pp. 1-30.
- [40] Zouain N. Some variational formulations of non-associated hardening plasticity. *Mechanics of Solids in Brasil* 2009, H.S. da Costa Mattos and M. Alves eds., *Brasilian Society of Mechanical Sciences and Engineering*, pp. 503-512. ISBN 978-85-85769-43-7.